SEQUENTIAL SOLUTIONS IN NONLINEAR CONTROL THEORY

By

BUCK FERGUSON BROWN

Bachelor of Science
Massachusetts Institute of Technology
Cambridge, Massachusetts
1955

Master of Science
Oklahoma State University
Stillwater, Oklahoma
1959

Submitted to the Faculty of the Graduate School of
the Oklahoma State University
in partial fulfillment of the requirements
for the degree of
DOCTOR OF PHILOSOPHY
May, 1964

SEQUENTIAL SOLUTIONS IN NONLINEAR

CONTROL THEORY

Thesis Approved:

Harold Freistor
Thesis Adviser

Paul A. McCollum

J. B. Boggs

E. J. Wallace

E. R. McLachlan

J. B. Boggs
Dean of the Graduate School

ACKNOWLEDGEMENT

I wish to take this opportunity to acknowledge my indebtedness to all members of the graduate committee composed of Professors H. T. Fristoe, P. A. McCollum, E. K. McLachlan, E. J. Waller, and J. H. Boggs. Their guidance and support have contributed much to the success of my studies.

I would also like to mention Professor N. W. McLachlan for kindling my interest in the analysis of nonlinear systems during his recent tenure as Visiting Professor on the Oklahoma State University campus. Finally, I would like to extend thanks to Professor J. R. Norton for providing the impetus for this research through his insight into the dynamics of physical systems.

TABLE OF CONTENTS

LIST OF TABLES

LIST OF FIGURES

LIST OF FIGURES (Continued)

CHAPTER I

INTRODUCTION

In recent years engineers have become vitally concerned with making better mathematical models for use in the analysis and synthesis of control systems. This concern is obviously an outgrowth of the general performance requirements and accuracies of modern technology. To the present much of analysis and synthesis has been based upon the powerful tool of linear systems theory with results which have proved nothing short of spectacular. It has become evident, however, that for wide ranges of operation some improvement is needed over the predictions of linear theory. In addition, it has been demonstrated that system response may be maximized according to some criteria such as rise time or steady state error through the purposeful introduction of nonlinearities (1). Investigations of such improvements have proceeded in only a limited manner, however, since in general the resultant ordinary nonlinear differential equations describing these systems do not have closed form solutions in terms of elementary functions.

This difficulty has been largely circumvented by using approximate solutions achieved through the partial sums of infinite series or through some numerical techniques. Indeed, the advent of high speed, high accuracy digital and analog computers has drastically modified the engineering concept of solutions for control systems described by such equations (2). In many cases the functional expression has been replaced by

continuous curves or even digitalized data and solution methods which heretofore have been considered too laborious to pursue, are now within practical grasp.

This thesis presents the results of a study based upon a method of linearizing certain nonlinear mathematical models of control systems. The solution obtained by this method is only approximate but the difference between this approximation and the actual solution is maintained within a specified tolerance.

There are several advantages to this method over some of the linearization techniques presently in wide use (3). Not the least of these is the possibility for the inclusion of arbitrary driving functions. In addition there is considerable similarity between the analysis of linear and nonlinear control systems as described here, resulting in a unification of approach.

The advantages mentioned are, however, not without sacrifice. In order to maintain reasonable accuracies the process of linearization must be repeated a great many times. The number being directly influenced by the degree of nonlinearity of the system under study and the time duration for which the solution is desired. Fortunately, this repetitious task may be relegated to the digital computer. Under these circumstances the sequential solution assumes many of the aspects of other numerical solution methods.

Of particular interest are the sections dealing with operational methods as applied to the linearized system. From consideration of the linearized equations it is possible to manipulate the block diagram equivalent of the nonlinear system provided that certain restrictions are adhered to unconditionally.

Transformation of the linearized equation into the complex frequency domain allows the characterization of the nonlinear system in terms of transfer function pole locations. It is demonstrated that nonlinear systems, unlike the linear counterpart, can have describing poles in the right half of the s-plane without having an unstable solution.

Consideration is also given to the operation of nonlinear systems as plants in closed loop control. The well known root locus technique is utilized to point the way toward obtaining desired response characteristics from these nonlinear devices.

CHAPTER II

SEQUENTIAL LINEARIZATION

The systems under investigation will be characterized by the universality of the model used for their representation. This mathematical description is assumed to be that of a nonlinear ordinary differential equation with canonical form (chosen for reasons soon to become apparent) as illustrated by equation II-1,

$$\frac{d^n x}{dt^n} + f_{n-1}(x) \frac{d^{n-1} x}{dt^{n-1}} + \ldots + f_1(x) \frac{dx}{dt} + f_0(x)\, x = F(t) \qquad \text{II-1}$$

having initial conditions at $t = t_0$ of

$$x = x_{10};\ \frac{dx}{dt} = x_{20};\ \ldots;\ \frac{d^{n-1} x}{dt^{n-1}} = x_{n0},$$

with functions $f_{n-1}(x)$, $f_{n-2}(x)$, ..., $f_0(x)$ and $F(t)$ all of class C^{1}[1] for $|x - x_{10}| \leq \beta$ and $|t - t_0| \leq \tau$.

Often it will be convenient to represent equation II-1 in terms of an equivalent system of n first-order ordinary differential equations (4,5) as shown by II-2 with x replaced by x_1.

---

[1] A function of a number of variables, $f = f(x_1, x_2, \ldots x_r)$, is said to be of class C^n in some region R when all of the derivatives $\frac{\partial f}{\partial x_i}, \frac{\partial^2 f}{\partial x_i \partial x_j}$ ..... of orders 1, $\cdots$, n exist and are continuous on R.

$$\begin{aligned}
\frac{dx_1}{dt} &= x_2 \\
\frac{dx_2}{dt} &= x_3 \\
&\vdots \\
\frac{dx_n}{dt} &= -x_1 f_0(x_1) - x_2 f_1(x_1) - \ldots - x_n f_{n-1}(x_1) + F(t)
\end{aligned} \qquad \text{II-2}$$

The system of II-2 has the normal form

$$\begin{aligned}
\frac{dx_1}{dt} &= G_1(x_1, x_2, \ldots, x_n, t) \\
&\text{- - - - - - - - - - - - - - - - -} \\
\frac{dx_n}{dt} &= G_n(x_1, x_2, \ldots, x_n, t)
\end{aligned} \qquad \text{II-3}$$

since there are n functions $G_1, G_2, \ldots, G_n$ of the n+1 variables $x_1, x_2, \ldots, x_n$ and t. These can be concisely written in terms of vector notation as

$$\frac{d\underline{x}}{dt} = \underline{G}(\underline{x}, t) \qquad \text{II-4}$$

where it is understood that $\underline{x}$ is an n-tuple, $\underline{x} = (x_1, x_2, \ldots, x_n)$. In addition the symbolism

$$\frac{d\underline{x}}{dt} = \underline{x}' \qquad \text{II-5}$$

shall be interpreted as

$$\frac{d\underline{x}}{dt} = \underline{x}' = (\underline{x}', \underline{x}_2', \ldots, \underline{x}_n') \qquad \text{II-6}$$

while $\underline{G}$ is a vector valued function of a vector variable and the real variable t as illustrated by equation II-7.

$$\underline{G}(\underline{x},t) = (G_1(x_1,x_2,\ldots,x_n,t),\ G_2(x_1,x_2,\ldots,x_n,t),\ldots \\ \ldots,G_n(x_1,x_2,\ldots,x_n,t)\ ) \qquad \text{II-7}$$

Comparison of equations II-2 and II-3 shows that each of the functions $G_1,G_2,\ldots,G_n$ and hence $\underline{G}$ is of class C^1 in any closed region, R, established such that $|x_1 - x_{10}| \leq \beta$ and $|t - t_0| \leq \tau$. $\underline{G}$ then satisfies a Lipschitz condition on R and for some finite constant, L

$$|\underline{G}(\underline{x},t) - \underline{G}(\underline{y},t)| \leq L|\underline{x} - \underline{y}| \qquad \text{II-8}$$

if $(\underline{x},t)$ and $(\underline{y},t)$ are in R.

The continuity of the derivative of $\underline{G}$ implies through equation II-8 that the vector differential equation II-4 defines a "well-set"[2] initial value problem. Thus there is the assurance that a solution to the system of equations exists which can be used to uniquely predict the future behavior of the model. This behavior in turn depends continuously upon the initial values.

A solution of II-4 shall be designated as $\underline{x}$ and will be associated with an initial condition point or vector

$$\underline{C} = (x_{10},x_{20},\ldots,x_{n0}) \qquad \text{II-9}$$

whose elements are simply the conditions specified at $t = t_0$ for equation II-1. The continuous nature of the vector function $\underline{G}(\underline{x},t)$ with

---

[2]Garrett Birkhoff and Gian-Carlo Rota, Ordinary Differential Equations (Boston, 1962), pp. 102-104.

respect to $\underline{x}$ and t implies that a solution $\underline{x}(t)$ of the vector integral equation

$$\underline{x}(t) = \underline{C} + \int_{t_0}^{t} \underline{G}(\underline{x}(r),r)dr \qquad \text{II-10}$$

is a solution of the vector differential equation II-4 which satisfies the initial condition $\underline{x}(t_0) = \underline{C}$, and conversely.[3] Here the meaning of the integral of a vector valued function is analogous to equation II-6.

$$\int_a^b \underline{G}(\underline{x}(r),r)dr = \left(\int_a^b G_1(\underline{x}(r),r)dr, \int_a^b G_2(\underline{x}(r),r)dr, \ldots, \int_a^b G_n(\underline{x}(r),r)dr\right) \qquad \text{II-11}$$

The Linear Model

Now suppose it happens as it often does in systems analysis, that the solution of II-1 is desired at a time, t = T, where

$$t_0 \leq T < \tau \ . \qquad \text{II-12}$$

Frequently it is necessary and sometimes perhaps even desirable to accept an approximate answer if the accuracy of such a value can be specified.

To generate an approximation of this nature, t_0 is assigned the specific value $t_0 = 0$ without loss of generality. If m and K are positive integers, $K \leq m$, let P_m be a partition of the closed interval $[0,T]$ such that the subinterval $[t_{K-1}, t_K]$ has length T/m. Construct a linearized system of equations for the subinterval corresponding to K = 1 such

[3] Ibid., p. 111.

that

$$\begin{aligned}
\frac{dy_1}{dt} &= y_2 \\
\frac{dy_2}{dt} &= y_3 \\
&\vdots \\
\frac{dy_n}{dt} &= -y_1 a_{10} - y_2 a_{11} - \cdots - y_n a_{1n-1} + F(t).
\end{aligned} \qquad \text{II-13}$$

In the system II-13 it is assumed that the constants a_{10}, a_{11}, ..., a_{1n-1} have been determined in accordance with II-14. The system may be represented

$$a_{10} = f_0(x_{10});\ a_{11} = f_1(x_{10});\ a_{12} = f_2(x_{10});\ \cdots;\ a_{1n-1} = f_{n-1}(x_{10}) \qquad \text{II-14}$$

in vector form as

$$\frac{d\underline{y}_1}{dt} = \underline{H}_1(\underline{y}_1, t). \qquad \text{II-15}$$

$\underline{H}_1(\underline{y}_1, t)$ is continuous and satisfies a Lipschitz condition on the interval $0 \leq t \leq t_1$ for all $\underline{y}_1$. Then the solution of II-15 which satisfies the initial condition, $\underline{C}$, of II-9 on this subinterval is

$$\underline{y}_1 = \underline{C} + \int_0^t \underline{H}_1(\underline{y}_1(r), r)\, dr \quad . \qquad \text{II-16}$$

For subintervals corresponding to $K \geq 2$, linearized systems similar to II-13 may be established. Thus for $t_{K-1} \leq t \leq t_K$ the system becomes

$$\frac{dy_1}{dt} = y_2$$

$$\frac{dy_2}{dt} = y_3$$

$$\vdots$$

$$\frac{dy_n}{dt} = -y_1 a_{K0} - y_2 a_{K1} - \cdots - y_n a_{Kn-1} + F(t)$$

where each of the constants $a_{K0}, a_{K1}, \cdots, a_{Kn-1}$ is formed in accordance with II-18. The value, $y_1(t_{K-1})$, is taken to be that obtained at the end

$$a_{K0} = f_0\left[y_1(t_{K-1})\right];\ a_{K1} = f_1\left[y_1(t_{K-1})\right];\cdots;a_{Kn-1} = f_{n-1}\left[y_1(t_{K-1})\right] \qquad \text{II-18}$$

point of the (K-1)th interval, $\left[t_{K-2}, t_{K-1}\right]$. The system II-17 may thus be written vectorially as

$$\frac{d\underline{y}_K}{dt} = \underline{H}_K(\underline{y}_K, t) \qquad \text{for } t_{K-1} \leq t \leq t_K. \qquad \text{II-19}$$

The intended task requires use of the unique solution of II-19 satisfying the initial condition

$$\underline{y}_K(t_{K-1}) = \underline{y}_{K-1}(t_{K-1}) \qquad \text{II-20}$$

as illustrated by II-21.

$$\underline{y}_K = \underline{y}_{K-1}(t_{K-1}) + \int_{t_{K-1}}^{t} \underline{H}_K(\underline{y}_K(r), r)dr \quad t_{K-1} \leq t \leq t_K \qquad \text{II-21}$$

Equation II-21 may be written in terms of the initial condition at $t = t_0$

as

$$\underline{y}_K = \underline{C} + \sum_{j=L}^{K-1} \int_{t_{j-1}}^{t_j} \underline{H}_j(\underline{y}_j(r),r)dr + \int_{t_{K-1}}^{t} \underline{H}_K(\underline{y}_K(r),r)dr \ . \qquad \text{II-22}$$

The first two terms of II-22 represent the initial condition at t_{K-1} and might properly be termed the "hereditary influences" of the Kth subinterval. These terms play a more significant role than that usually associated with initial conditions, however; since the first component of these "hereditary" terms is employed through equations II-18 to determine the linearized vector integrand, $\underline{H}_K$, of the remaining term on the right side of II-22.

From II-22 it is apparent that $\underline{y}_K$ is a continuous function within each subinterval for $1 \leq K \leq m$. The union of the $\underline{y}$ for $1 \leq K \leq m$ is continuous and is defined throughout the interval

$$t_0 \leq t \leq T. \qquad \text{II-23}$$

It will be convenient from this point to designate this union of $\underline{y}_K$ as $\underline{y}$. The use of this symbol will henceforth be restricted to the

$$\underline{y} = \bigcup_{K=1}^{m} \underline{y}_K \qquad \text{II-24}$$

solutions, $\underline{y}_K$, for $1 \leq K \leq m$ of the system of equations represented by II-17 and II-19 provided that the "hereditary terms" are used to constitute the initial conditions in each case. In addition it is noted that $\underline{y}$ will be referred to as a <u>sequential solution</u> of the nonlinear system II-2 which satisfies the initial condition $\underline{C}$. Finally the sequential solution, $\underline{y}$ will be said to be <u>based</u> upon the systems of equations II-19.

If the sequential solution, $\underline{y}$, is to be of utility, it will possess the same initial condition, $\underline{C}$, at t_0 as the solution, $\underline{x}$, of the non-linear system II-4. Furthermore for every t where

$$t_0 \leq t \leq T \qquad \text{II-25}$$

the solutions must differ to only a slight extent.

The sequential solutions formed from the union of $\underline{y}_K$ for integer values of m constitute a sequence of functions. This sequence converges uniformly to $\underline{x}$ on the interval of II-25 since for every $\epsilon > 0$, there exists an M depending only on ϵ such that $m > M$ implies

$$\left| \underline{x} - \bigcup_{K=1}^{m} \underline{y}_K \right| < \epsilon \quad . \qquad \text{II-26}$$

To verify this uniform convergence consider the following development.

Let $\underline{y}$ and $\underline{x}$ satisfy the differential equations

$$\frac{d\underline{y}}{dt} = \underline{H}_K(\underline{y},t) \text{ and } \frac{d\underline{x}}{dt} = \underline{G}(\underline{x},t) \qquad \text{II-27}$$

respectively on the Kth subinterval of II-25. $\underline{G}$ satisfies a Lipschitz condition on this subinterval. Let L be a Lipschitz constant associated with this vector function. Form a real valued function, $\sigma(t)$, defined on the identical subinterval such that

$$\sigma(t) = \left| \underline{x} - \underline{y} \right|^2. \qquad \text{II-28}$$

The function $\sigma(t)$ is differentiable and its derivative can be written as

$$\frac{d\sigma}{dt} = 2 \left[\underline{x} - \underline{y} \right] \cdot \left[\frac{d\underline{x}}{dt} - \frac{d\underline{y}}{dt} \right] , \qquad \text{II-29}$$

or

$$\frac{d\sigma}{dt} = 2\left[\underline{x}-\underline{y}\right]\left[\underline{G}(\underline{x},t)-\underline{H}_K(\underline{y},t)\right]$$
$$= 2\left[\underline{x}-\underline{y}\right]\left[\underline{G}(\underline{x},t)-\underline{G}(\underline{y},t)\right] \qquad \text{II-30}$$
$$+ 2\left[\underline{x}-\underline{y}\right]\left[\underline{G}(\underline{y},t) - \underline{H}_K(\underline{y},t)\right]$$

The factor $\left[\underline{G}(\underline{y},t) - \underline{H}_K(\underline{y},t)\right]$ of II-30 is defined only on the domain common to both functions. Since the domain, D, of $\underline{H}_K$ is by its very definition a subset of the domain of $\underline{G}$ it follows that if $\underline{Z}$ is in D there exists a $\Delta_K > 0$ such that

$$\left|\underline{G}(\underline{Z},t) - \underline{H}_K(\underline{Z},t)\right| \leq \Delta_K \ . \qquad \text{II-31}$$

Application of the Lipschitz condition which $\underline{G}$ satisfies along with II-31 yields

$$\left|\frac{d\sigma}{dt}\right| \leq 2L\left|\underline{x}-\underline{y}\right|^2 + 2\Delta_K\left|\underline{x}-\underline{y}\right| \ , \qquad \text{II-32}$$

or

$$\frac{d\sigma}{dt} \leq 2L\sigma(t) + 2\Delta_K\sqrt{\sigma(t)} \ . \qquad \text{II-33}$$

Now comparison[4] of II-33 with a Bernoulli[5] differential equation such as that of II-34

$$\frac{du}{dt} = 2\Delta_K\sqrt{u} + 2Lu \qquad u \geq 0 \qquad \text{II-34}$$

having a solution

$$\sqrt{u(t)} - \sqrt{u(t_{u-1})}\ e^{L(t-t_{K-1})} + \left(\frac{\Delta_K}{L}\right)\left(e^{L(t-t_{K-1})}-1\right), \qquad \text{II-35}$$

which satisfies the initial condition $u(t_{K-1}) = \sigma(t_{K-1})$, results in

---

[4] Birkhoff and Rota, pp. 106-107

[5] E. L. Ince, Ordinary Differential Equations (Dover ed., 1956), p. 22.

the inequality

$$\left| \underline{x}(t) - \underline{y}(t) \right| \leq \left| \underline{x}(t_{K-1}) - \underline{y}(t_{K-1}) \right| e^{L \left| t-t_{K-1} \right|} + \frac{\Delta_K}{L} \left[e^{L \left| t-t_{K-1} \right|} - 1 \right] \qquad \text{II-36}$$

At the end point of the Kth subinterval then this difference may be expressed as

$$\left| \underline{x}(t_K) - \underline{y}(t_K) \right| \leq \left| \underline{x}(t_{K-1}) - \underline{y}(t_{K-1}) \right| e^{LT/m} + \frac{\Delta_K}{L} \left[e^{L/Tm} - 1 \right] \qquad \text{II-37}$$

The difference, $\left| \underline{x}(t_K) - \underline{y}(t_K) \right|$, can be related to preceding subintervals through the factor, $\left| \underline{x}(t_{K-1}) - \underline{y}(t_{K-1}) \right|$, in the manner of II-37 as

$$\left| \underline{x}(t_{K-1}) - \underline{y}(t_{K-1}) \right| \leq \left| \underline{x}(t_{K-2}) - \underline{y}(t_{K-2}) \right| e^{LT/m} + \frac{\Delta_{K-1}}{L} \left[e^{LT/m} - 1 \right] \qquad \text{II-38}$$

Let Δ designate the largest of the set of differences, $\{\Delta_i\}$, encountered in any of the subintervals. Then repeated application of II-38 allows II-37 to be written as

$$\left| \underline{x}(t_K) - \underline{y}(t_K) \right| \leq \sum_{i=1}^{K} \left(\frac{\Delta}{L} \left[e^{LT/m} - 1 \right] e^{(m-i)LT/m} \right) \qquad \text{II-39}$$

Each of the terms of the summation on the right side of II-39 is greater than zero and hence the greatest difference can occur at t = T. This corresponds to the subinterval K = m so that inequality II-39 may be written as

$$\left| \underline{x}(T) - \underline{y}(T) \right| \leq \sum_{i=1}^{m} \left(\frac{\Delta}{L} \left[e^{LT/m} - 1 \right] e^{(m-i)LT/m} \right). \qquad \text{II-40}$$

From II-40 it then is apparent that

$$\left| \underline{x}(T) - \underline{y}(T) \right| \leq \frac{\Delta_m}{L} \left[e^{LT/m} - 1 \right] e^{LT} \quad . \qquad \text{II-41}$$

The right side of II-41 has the factor

$$f_m = m\left[e^{LT/m} - 1\right] = \left[e^{LT/m}-1\right] \Big/ \left(\frac{1}{m}\right);\ LT>0 \qquad \text{II-42}$$

which for positive integer values of m forms a monotonic decreasing sequence. The infimum of the sequence is

$$LT = \inf\left\{f_m\right\} \qquad \text{II-43}$$

while the supremum is

$$\left[e^{LT}-1\right] = \sup\left\{f_m\right\} . \qquad \text{II-44}$$

It becomes convenient to replace $\sup\left\{f_m\right\}$ with the upper bound e^{LT} and write the inequality II-41 as

$$\left|\underline{x}(T) - \underline{y}(T)\right| < \Delta\cdot\frac{e^{2LT}}{L} . \qquad \text{II-45}$$

Thus it may be concluded from II-45 that the maximum difference (henceforth denoted as the maximum sequential solution error) between the solution, $\underline{x}$, of the nonlinear equation and the sequential solution, $\underline{y}$, within the time interval

$$0 = t_0 \leq t \leq T \qquad \text{II-46}$$

does not exceed $\Delta\cdot(e^{2LT}/L)$. As might be expected for any nonlinear differential equation with canonical form illustrated by II-1, the maximum sequential solution error increases with the length of the t-interval under consideration. For any particular differential equation having this canonical form, however, a finite Lipschitz constant greater than zero exists and hence for finite values of T the factor, (e^{2LT}/L), exists.

It remains to be shown that Δ can be made arbitrarily small by simply increasing the total number of subintervals, m. This is accomplished from consideration of the quantity

$$\delta_{KM} = \left| \underline{G}(y_K, t) - \underline{H}_K(y_K, t) \right| \qquad \text{II-47}$$

This relationship reduces to

$$\delta_{KM} = \left| y_1 \left[a_{K0} - f_0(y_1) \right] + y_2 \left[a_{Ki} - f_1(y_1) \right] + \ldots + y_n \left[a_{Kn} - f_n(y_1) \right] \right| \qquad \text{II-48}$$

which at the beginning of the Kth interval ($t = t_K$) has a value $\delta_{KM} = 0$, by virtue of the defining relation for each of the constants, a_{Ki}. Within this interval y_1 is a continuous function of the scalar variable t and so, too, is each of the factors

$$\left[a_{Ki} - f_i(y_1) \right] . \qquad \text{II-49}$$

The derivative of this factor is

$$\frac{d\left[a_{Ki} - f_i(y_1) \right]}{dt} = - \frac{df_i(y_1)}{dy_1} \cdot y_2 \qquad \text{II-50}$$

where i is an integer such that $1 \leq i \leq n$.

Let the maximum magnitude of the absolute value of this derivative with respect to y_1 for any i as exists on the region of definition, R, be designated as

$$f'_{max} = \left| \frac{df_i(y_1)}{dy_1} \right| \qquad \text{II-51}$$

From this then it is clear that

$$\left| \left[a_{Ki} - f_i(y_1) \right] \right| \leq f'_{max} \cdot \left| y_2 \right| \cdot T/m \qquad \text{II-52}$$

at any point of the subinterval of length T/m. Application of the triangle inequality to II-48 yields

$$\delta_{KM} \leq |y_1| \cdot |a_{K0} - f_0(y_1)| + |y_2| \cdot |a_{Ki} - f_1(y_1)| + \ldots + |y_n| \cdot |a_{Kh} - f_n(y_1)| \qquad \text{II-53}$$

For m = M through the utilization of II-52 the inequality II-53 becomes

$$\delta_{KM} \leq |y_1| \cdot |y_2| f'_{max} T/M + |y_2| \cdot |y_2| f'_{max} T/M + \ldots + |y_n| \cdot |y_2| f'_{max} T/M . \qquad \text{II-54}$$

The values of the vector variable, $\underline{y}$, are a subset of the closed region R and hence there exists some positive value Q such that

$$|\underline{y}| < Q. \qquad \text{II-55}$$

Each of the components of $\underline{y}$ is less than Q as is symbolized in II-56 with i an integer such that $1 \leq i \leq n$.

$$|\underline{y}_i| < Q. \qquad \text{II-56}$$

Consideration of II-54 and II-56 leads to

$$\delta_{KM} < nQ^2 f'_{max}(T/M). \qquad \text{II-57}$$

Furthermore it is recognized that Δ is the maximum value of δ_{KM} as K is allowed to range from 1 to M and so it may be written that

$$\Delta < nQ^2 f'_{max}(T/M) \qquad \text{II-58}$$

Clearly for m>M this leads to

$$\Delta < nQ^2 f'_{max}(T/m) < nQ^2 f'_{max}(T/M). \qquad \text{II-59}$$

In accordance with II-26 let

$$\epsilon = \triangle(e^{2LT}/L). \qquad \text{II-60}$$

Then the sequential solution converges uniformly on the interval of II-25. In addition it is noted that the limit function is $\underline{x}$, the solution of the nonlinear differential equation under consideration. Thus it can be said that the sequential solution differs by less than ϵ from the actual solution as is depicted by equation II-61.

$$\left| \underline{x} - \underline{y} \right| < \triangle e^{2LT}/L \qquad \text{II-61}$$

CHAPTER III

OPERATIONAL METHODS AND THE SEQUENTIAL SOLUTION

The preceding chapter has established a method for linearizing a nonlinear ordinary differential equation of the form shown in II-1. In addition it has been demonstrated that the maximum error encountered through this procedure cannot only be calculated but also regulated simply by the selection of the number of subintervals, m, upon which the sequential solution is based.

The benefits to be derived from use of the sequential solution are many. It becomes immediately apparent that the solution of nonlinear engineering systems as described by II-1 (and there are a great many) has been reduced to the repeated solution of linear ordinary differential equations of the same order as the original nonlinear equation. The disadvantage encountered in this technique is also readily observed in that the solution accuracy is inversely proportional to the number of subintervals involved. Such repeated calculations are well suited to manipulation on a digital computer and are limited in accuracy only by the inherent accuracies of the computing machine.

The operational methods of analysis described here are restricted to the extension of the well known linear system methods involving the Laplace Transformation. This is of importance since the incremental system of II-17, repeated here as III-1 for convenience, can be

$$\begin{aligned}
\frac{dy_1}{dt} &= y_2 \\
\frac{dy_2}{dt} &= y_3 \\
&\vdots \\
\frac{dy_n}{dt} &= -y_1 a_{K0} - y_2 a_{K1} - \ldots - y_n a_{Kn-1} + F(t)
\end{aligned} \qquad \text{III-1}$$

rewritten in terms of the equivalent nth order linear equation III-1 becomes

$$\frac{d^n y}{dt^n} + a_{Kn-1}\frac{d^{n-1} y}{dt^{n-1}} + a_{Kn-2}\frac{d^{n-2} y}{dt^{n-2}} + \ldots + a_{K0} y = F(t) \qquad \text{III-2}$$

where y_1 has been replaced by y. The transformation of this equation in terms of the complex variable, s, is accomplished by letting $t = u + t_{K-1}$ and yields

$$\begin{aligned}
Y(s)\left[s^n + a_{Kn-1}s^{n-1} + a_{Kn-2}s^{n-2} + \ldots + a_{K1}s + a_{K0}\right] = \\
s^{n-1}y_1(t_{K-1}) + s^{n-2}\left[y_2(t_{K-1}) + a_{Kn-1}y_1(t_{K-1})\right] + s^{n-3}\left[y_3(t_{K-1}) + \right. \\
\left. a_{Kn-1}y_2(t_{K-1}) + a_{Kn-2}y_1(t_{K-1})\right] + \ldots + \left[y_n(t_{K-1}) + \right. \\
\left. a_{Kn-1}\, y_{n-1}(t_{K-1}) + \ldots + a_{K1}y_1(t_{K-1})\right] + \mathcal{L}\left\{F(u + t_{K-1})\right\}
\end{aligned} \qquad \text{III-3}$$

Solution of III-3 for Y(s) can be considered as consisting of two component parts. The first of these, designated $Y_1(s)$, is specified by III-4 and is due to the initial condition terms. The second component,

$$Y_1(s) = \frac{N(s)}{s^n + a_{Kn-1}s^{n-1} + a_{Kn-2}s^{n-2} + \ldots + a_{K1}s + a_{K0}} \qquad \text{III-4}$$

where

$$N(s) = s^{n-1}y_1(t_{K-1}) + s^{n-2}\left[y_2(t_{K-1}) + a_{Kn-1}y_1(t_{K-1})\right] + \cdots$$

$$\cdots + \left[y_n(t_{K-1}) + a_{Kn-1}y_{n-1}(t_{K-1}) + \cdots + a_{K1}y_1(t_{K-1})\right]$$

$Y_2(s)$, is a result of the forcing function and may be written as

$$Y_2(s) = \frac{\mathcal{L}\left\{F(u + t_{K-1})\right\}}{s^n + a_{Kn-1}s^{n-1} + a_{Kn-2}s^{n-2} + \cdots + a_{K1}s + a_{K0}} . \quad \text{III-5}$$

The solution for Y(s) in terms of the components is

$$Y(s) = Y_1(s) + Y_2(s) \quad \text{III-6}$$

Thus in the Kth subinterval the solution of the nonlinear equation and the inverse transform of III-6 are such that

$$|x - y| < \Delta(e^{2LT}/L) \quad \text{III-7}$$

where here it is assumed that $x = x_1$ and $y = y_1$ are components of the vectors $\underline{x}$ and $\underline{y}$ which satisfy the inequality II-61 with $t_0 \leq t \leq T$.

From III-4 and III-5 the importance of the characteristic polynomial

$$s^n + a_{Kn-1}s^{n-1} + a_{Kn-2}s^{n-2} + \cdots + a_{K1}s + a_{K0} \quad \text{III-8}$$

is quite evident. The inverse transform of the component $Y_1(s)$ is wholly dependent upon the roots of this polynomial for its form. The second component, $Y_2(s)$, has an inverse which also depends in large part upon the characteristic polynomial roots but it relies in addition upon the roots of the factors found in the denominator of the transform of F(t).

The Root Ensemble

Because of their position of importance it becomes expedient to investigate the characteristic roots in some detail. This will be accomplished in part by considering the locations of the roots on the complex or s-plane. These locations depend upon the various coefficients, a_{Ki}, which are generally contingent upon the value of K. To alleviate the problem of describing the root locations in a sequential fashion it is useful to simply show all of the root locations possible for the region, R. Since this with all such roots taken together provides a description of the nonlinear differential equation, it is convenient to designate them as the root ensemble.

The root ensemble possesses certain definitive qualities which are outlined here. The first of these is a consequence of the canonical form chosen for the mathematical model of the nonlinear systems under investigation. In accordance with equation II-1, the coefficient of the highest derivative is unity. It follows therefore that although the linear system coefficients, a_{Ki}, from the base of the sequential solution may vanish, there will always be an nth derivative present. The transformed equation within each subinterval then has n roots. These are not necessarily distinct and so it is required that a root of multiplicity, r, be included as r roots.

The n roots which exist may either be real or complex. Since each of the a_{Ki} is restricted to real values, the complex roots which do occur must appear in complex conjugate pairs. Furthermore as the value of y is allowed to vary throughout the region of definition of the coefficient functions, $f_i(x)$, of II-1 the root locations will be altered.

The path which each root traces will be denoted a branch so that the nonlinear equation II-1 will have associated with it a root ensemble of n branches. Obviously, for each branch or section of branch located above the real axis in the s-plane there is a corresponding branch or portion of a branch below the axis. In short, the root ensemble possesses symmetry about the real axis as the branches appear in complex conjugate pairs. At the beginning of the Kth subinterval where $y = y(t_{K-1})$ a set of n root locations can be determined which in transfer function form represent the ratio of the quantities $Y_2(s)$ and the transformed driving function, $\mathcal{L}\{F(u + t_{K-1})\}$. If, in addition, the initial conditions at $t = t_{K-1}$ $(u = 0)$ are inserted properly, this transfer function may be utilized during the Kth subinterval for the purpose of block diagram manipulation and system analysis. Figure 1 shows a Kth subinterval linearized nth order system with the appropriate initial conditions.

Practical application of the root ensemble to the analysis of control systems requires that $\underline{y} = 0$ be included within the region, R, almost without exception. This in turn implies that $\underline{x} = 0$ is contained in R. If $F(t) = 0$ for all t such that $|t - t_0| \leq \tau$ then $\underline{x} = 0$ is a singular point of II-2. This situation is of particular interest since it is generally desirable to approach zero output, $x = 0$, for large values of t when $F(t) = 0$. According to linear theory this represents a stable system. In order to maintain this desirable operating mode it is essential that the derivatives of x also tend to zero.

Unless otherwise specified, root ensembles will be shown with branches eminating from the root locations corresponding to $y = 0$. Arrows will be directed away from these points and are merely intended

to illustrate the progression of the characteristic roots upon which the sequential solution is based as y increases or decreases. It cannot be overemphasized that the arrow directions do not imply anything with regard to the location of the roots for increasing values of time. The root ensemble is independent of time and the sequential manner in which root selection is made depends entirely upon the system response to the initial conditions and forcing function associated with each of the subintervals.

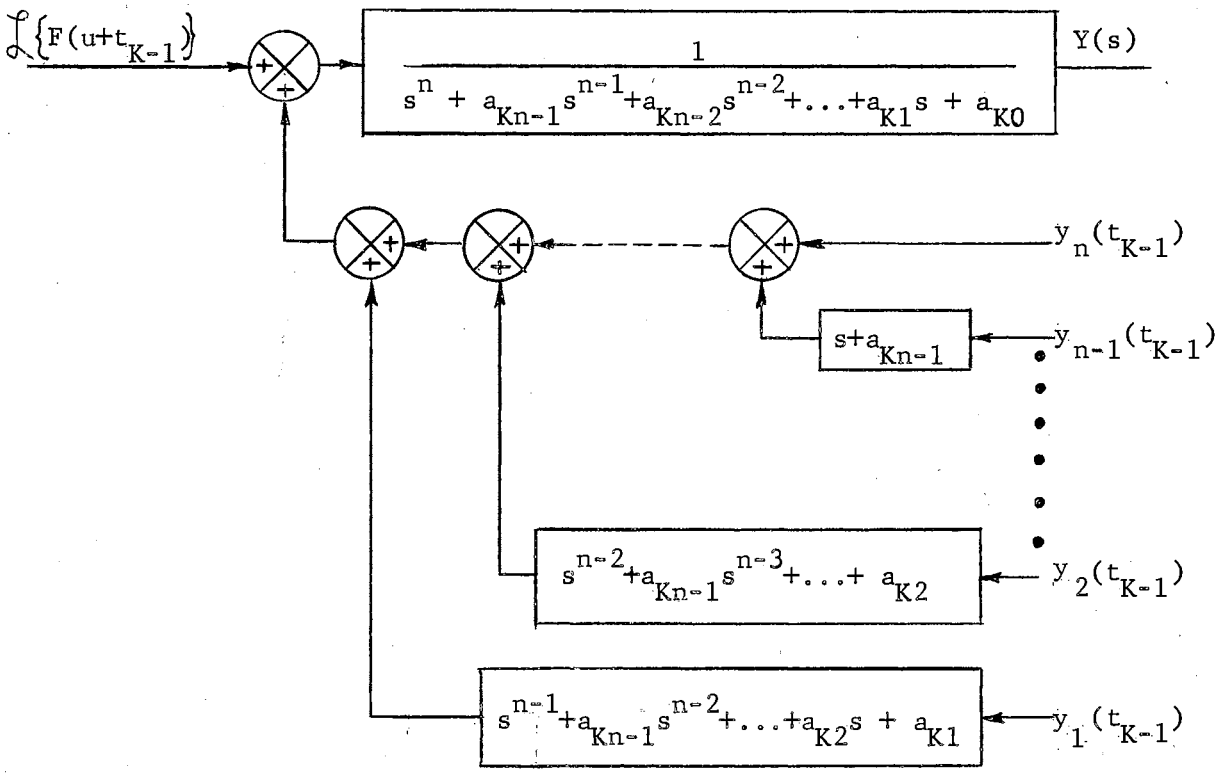

Figure 1. Block Diagram Representation of the Nonlinear System Within the Kth Subinterval

A cursory glance at a root ensemble leaves the impression that it greatly resembles the conventional linear system root locus. Indeed there is considerable similarity, but the likeness is more predominant in outward appearances than in actuality.

In direct contrast to the root locus, the root ensemble is not restricted to closed loop system analysis. It is equally applicable to open loop control provided only that the system being investigated has a mathematical model as described by equation II-1.

This endeavor will concentrate on the closed loop aspect since self-correcting methods are usually deemed superior to other available techniques of control. Two major categories immediately manifest themselves. The first of these (category I) is characterized by a closed loop system equation of the form of II-1. The second and equally interesting case (category II) is that in which the forward transmission is governed by this same relationship.

Figures 2 through 10 illustrate three nonlinear systems and their root ensembles. The first two of these systems are distinguished by the fact that only the closed loop equations are of the prescribed form. A more detailed consideration of these systems as presented in Appendix A indicates a considerable difference between the first and second of these in spite of the previously described similarity. Thus category I systems may be further subdivided into those with mathematical models of the form of II-1 only if no driving function (similar to the one illustrated in Figure 2) is present and those possessing this mathematical model without regard for the presence of the driving function (similar to that shown in Figure 5).

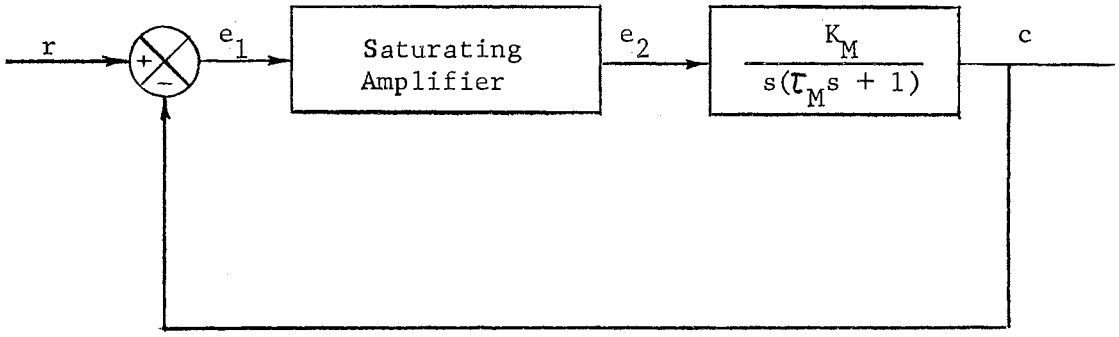

Figure 2. A Nonlinear Closed Loop Control System

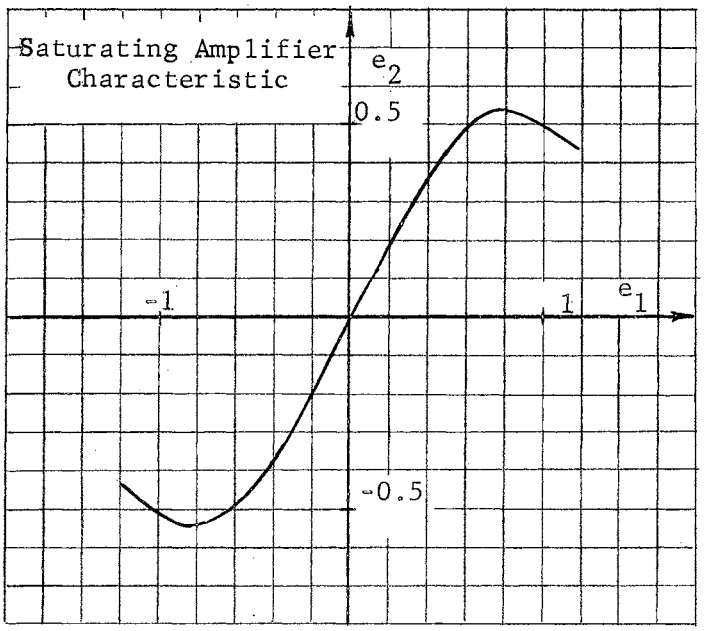

Figure 3. The Relationship Between the Amplifier Input and Output

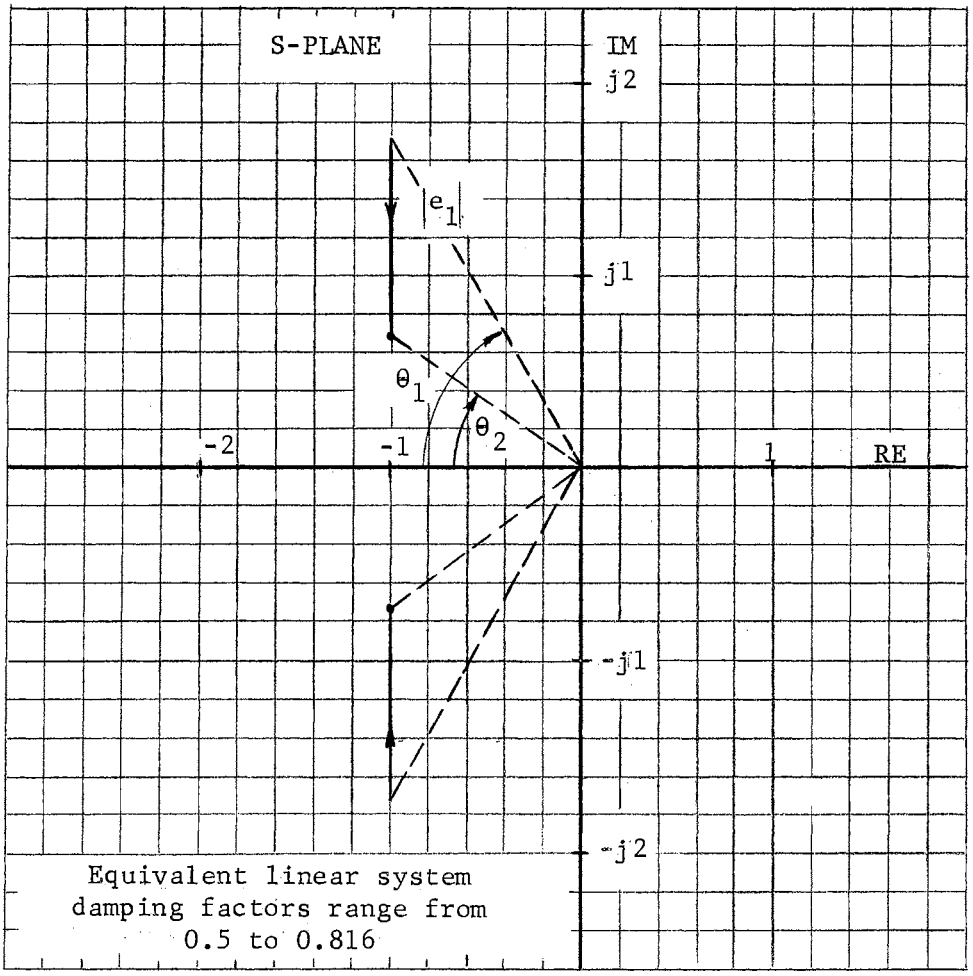

Figure 4. Root Ensemble of Positional Control System with Saturating Amplifier

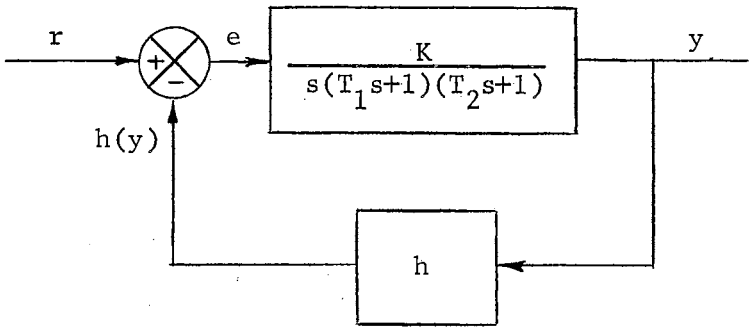

Figure 5. Control System with Nonlinear Feedback Element

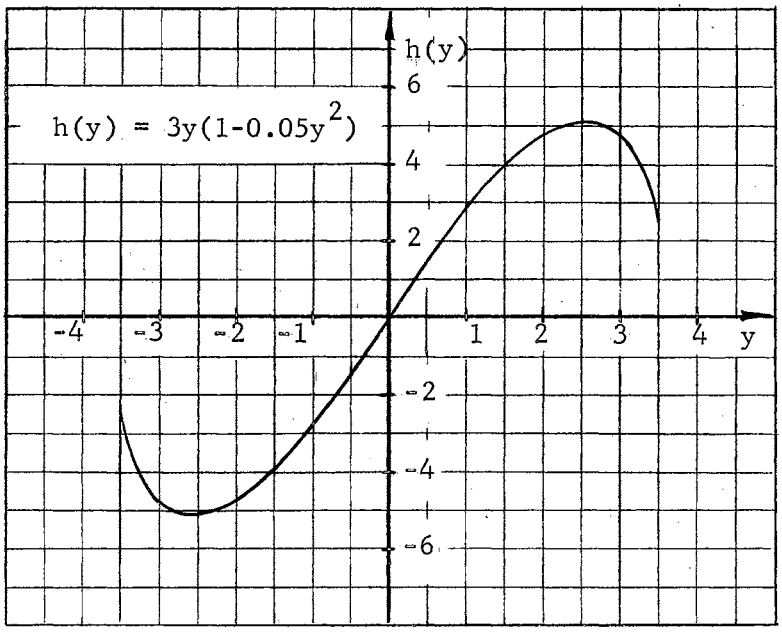

Figure 6. Nonlinear Feedback Element Characteristic

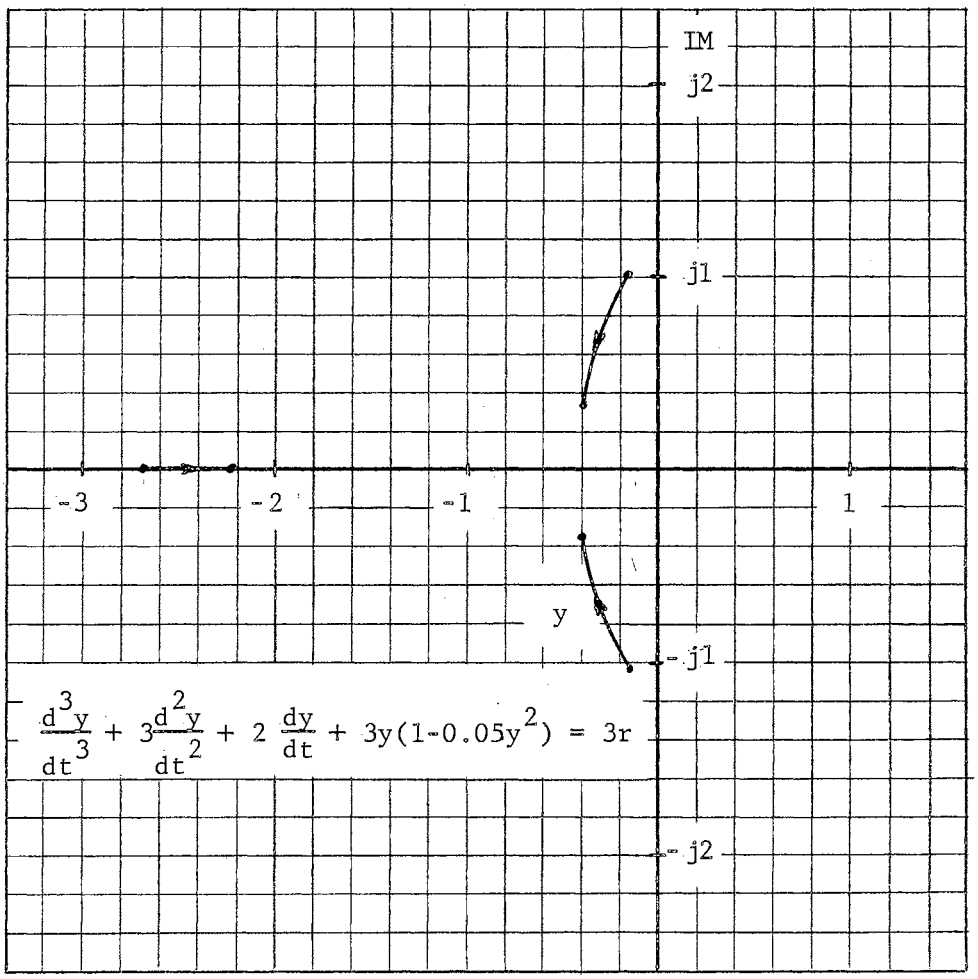

Figure 7. Root Ensemble of Control System with Nonlinear Feedback Element

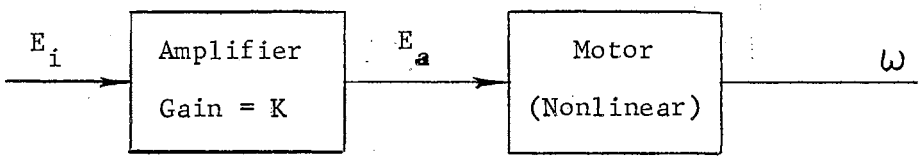

Figure 8. A Nonlinear Speed Control System

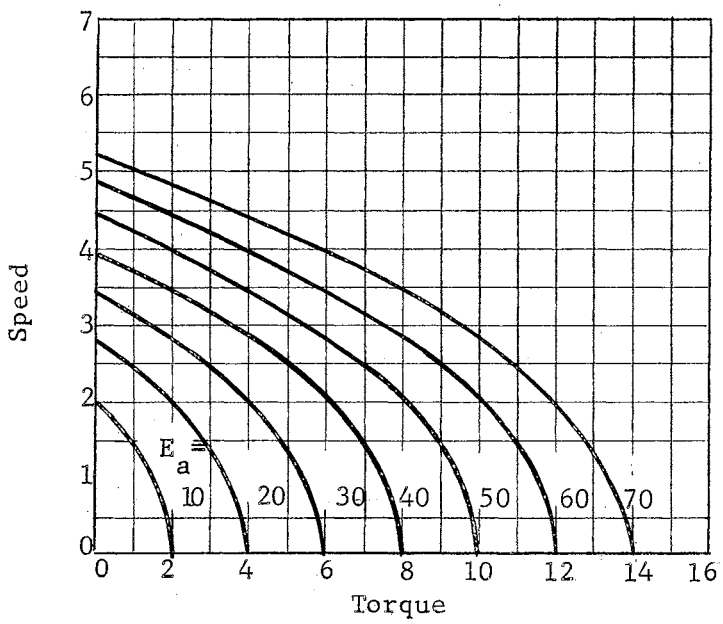

Figure 9. Motor Speed-Torque Characteristic

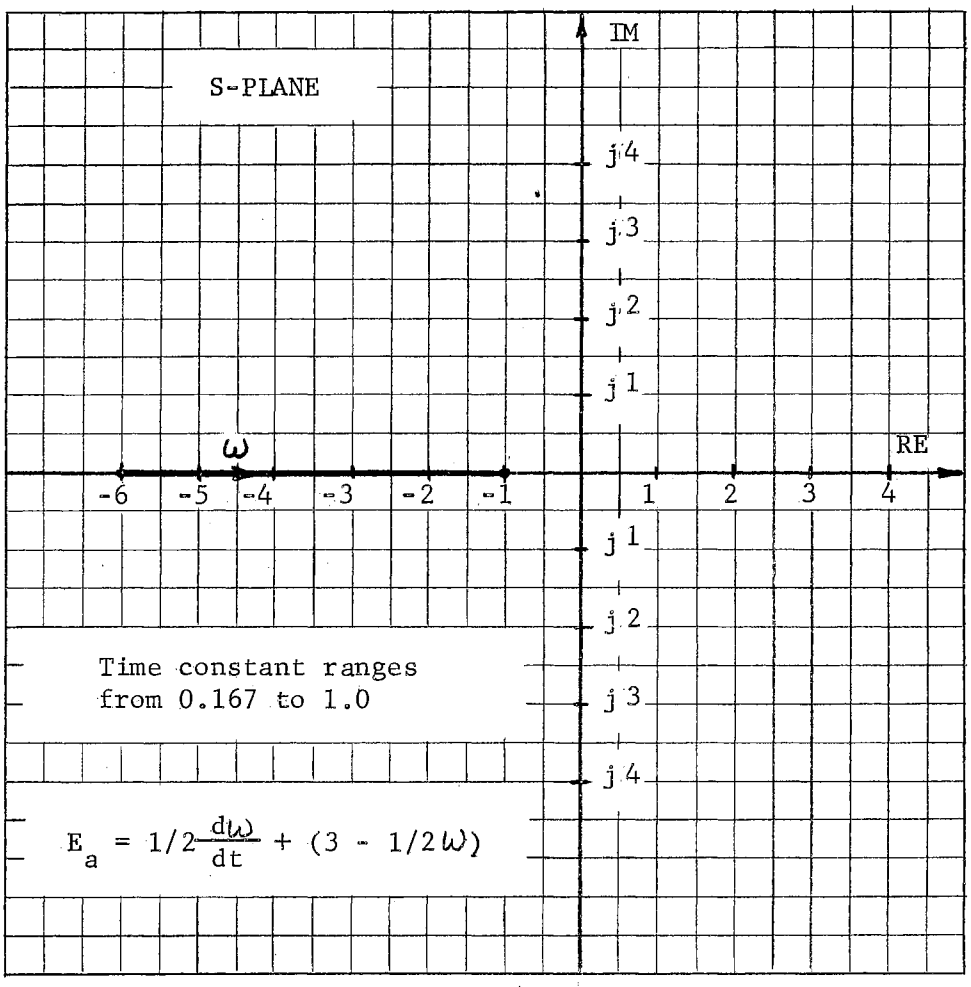

Figure 10. Root Ensemble for Nonlinear Speed Control System

Figure 8 is representative of a forward transmission path of a category II system since this open loop amplifier-motor combination is described by an equation of the form of II-1. It should be pointed out here that category I systems of the second variety may serve as forward transmission paths for category II systems. A discussion of the further properties of category II systems will be delayed until Chapter V. This is in order that some of the more general characteristics of both category I and II systems may be developed.

In future references to category I systems it will in general be clear from the context of the material under consideration whether or not both varieties are intended to be included. In those few places where some question exists an explicit statement will be incorporated as to its essence.

Block Diagram Algebra

Figure 1 suggests that many of the problems of nonlinear systems theory might be handled through the use of conventional block diagram techniques. The ultimate goal of any such scheme would be to provide methods for not only analyzing but also synthesizing systems having certain desired qualities. Unfortunately the use of block diagram algebra falls far short of these goals. Even so, some benefit is derived from the conceptual aspects of block diagram representation.

From the beginning it is convenient to separate the process of analysis from that of synthesis. The reason for this sharp division becomes evident after consideration of some of the fundamental block operations encountered in analysis. Without exception the intent of these operations is to simplify and thus find an equivalent configuration

which may be handled with greater ease.

There are two requirements which a manipulation must meet if it is to result in a suitable equivalent system diagram. First, the driving points for the nonlinear portion or portions of the diagram must remain unaltered throughout the simplification and second, the output point or points from these same nonlinear segments must be kept as distinct locations. Both of these conditions arise from the nature of the linearized system of Figure 1. Clearly any alteration in the driving points results in a modification of the actual forcing function involved in the nonlinear system equation. In view of the dependent nature of the linearized system's coefficients, a_{Ki}, upon the response y, regulation of this input to only proper values is critical. Further the output value, y, must be known so as to provide for the correct linearized model during succeeding subintervals.

Figure 11 represents a nonlinear system (either category I or II) cascaded both to the left and right with several linear devices each having transfer functions as shown. These linear elements have been combined in Figure 12 in accordance with the necessary conditions. The implications are clear from these figures. Normal block diagram manipulation may occur in a system containing nonlinearities while still maintaining equivalence provided that

1. linear elements are combined in the proper and well known manner,
2. each nonlinear portion of the system along with its input and output stations is maintained as an entity, and
3. the succession of linear and nonlinear elements is preserved.

The conditions set forth above preclude the possibility of rearranging the blocks whenever one of them is nonlinear. Another restriction immediately apparent is that summing and/or pick-off junctions may not be moved past any nonlinearity.

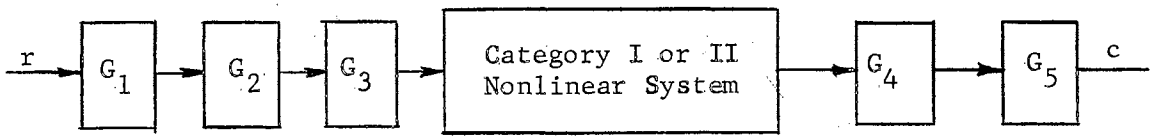

Figure 11. A Control System Consisting of Cascaded Linear and Nonlinear Segments

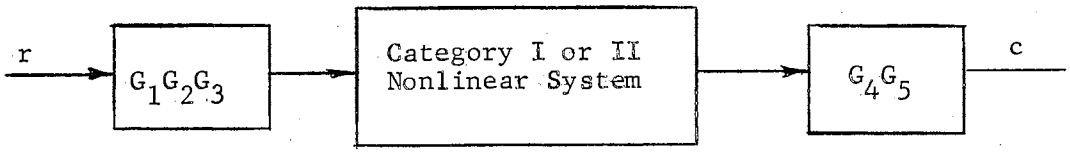

Figure 12. Simplified Equivalent of Preceding System Made Possible Through Combination of Linear Elements

All of these limitations seriously restrict the usefulness of block diagram algebra in the realm of nonlinear systems analysis. In direct contrast is its utility in the process of system synthesis. The mathematical goals involved in synthesis are somewhat different than those of analysis. It will be assumed for present purposes that certain system characteristics are desired and that these must be achieved with

nonlinear plants. These plants in turn will be restricted either to category I or II. Under these circumstances the synthesis procedures actually reduce to the techniques of compensation. From this point investigations proceed naturally toward closed loop methods.

The condition of manipulation associated with analysis are not directly applicable in synthesis since system simplification and equivalence are not the primary intent. Linear and nonlinear components may be interchanged at will while summing and/or pick-off points may be located at any desired station. Of course an awareness must be kept of consequences of such modifications.

Unlimited combinations of linear and nonlinear elements exist which may be brought together possibly resulting in a system conformable to the specifications. However, practical considerations such as power handling capabilities and overall range of operation narrow the placement of linear compensating devices to feedback paths and positions preceding the nonlinear plant.

Figures 13 and 14 represent such a compensation scheme. In each diagram the block designated G(s) or H(s) is a linear system transfer function consisting of polynomials (N(s) and D(s)) in s with real coefficients in both numerator and denominator. G(s) may be written as

$$G(s) = \frac{K_1 N_1(s)}{D_1(s)} = \frac{K_1 \left[S^w + C_{w-1} S^{w-1} + C_{w-2} S^{w-2} + \ldots + C_1 S + C_0 \right]}{S^v + b_{v-1} S^{v-1} + b_{v-2} S^{v-2} + \ldots + b_1 S + b_0} \qquad \text{III-9}$$

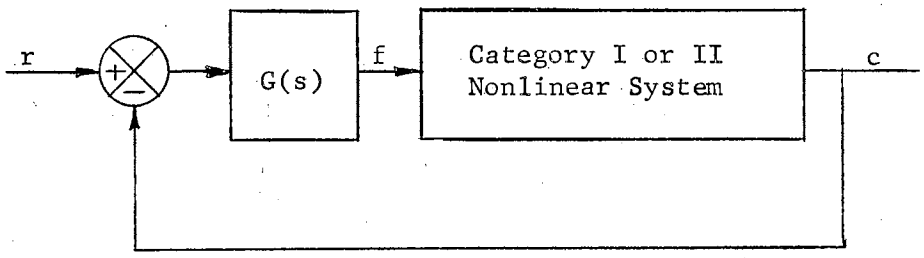

Figure 13. Forward Transmission Compensation of A Nonlinear Feedback System

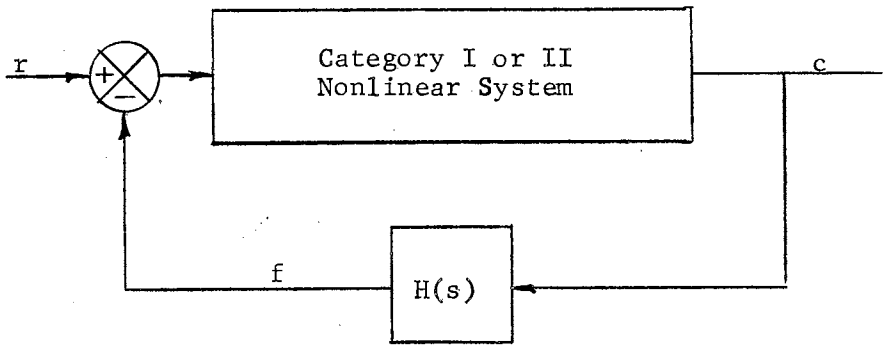

Figure 14. Compensation in the Feedback Path of A Nonlinear Closed Loop Control System

and H(s) as

$$H(s) = \frac{K_2 N_2(s)}{D_2(s)}$$

$$= \frac{K_2 \left[s^q + e_{q-1} s^{q-1} + e_{q-2} s^{q-2} + \ldots + e_1 s + e_0 \right]}{s^p + d_{p-1} s^{p-1} + d_{p-2} s^{p-2} + \ldots + d_1 s + d_0} \quad \text{III-10}$$

Consider the system of Figure 13. During the Kth subinterval let $t = u + t_{K-1}$. The input driving function to the nonlinear portion of

this system is

$$F(u + t_{K-1}) = \mathcal{L}^{-1}\left\{R_K(s)G(s) - Y(s)G(s)\right\} \qquad \text{III-11}$$

where

$$R_K(s) = \int_{u=0}^{\infty} r(u + t_{K-1})\, e^{-su}\, du + \Big\{ s^{v-1} f_1(t_{K-1}) + s^{v-2}\left[f_2(t_{K-1}) + b_{v-1}\, f(t_{K-1})\right] + \ldots + \left[f_v(t_{K-1}) + b_{v-1} f_{v-1}(t_{K-1}) + \ldots + b_1\, f_1(t_{K-1})\right]\Big\} \qquad \text{III-12}$$

and $f_i = \dfrac{d^{i-1}f}{dt^{i-1}}$ is the i-1 derivative of the output of the linear compensating device. Transformation of the incrementally linearized equation of the nonlinear portion of the system results in the relationship III-3 with $F(u + t_{K-1})$ replaced by III-11. The solution for Y(s) is then

$$Y(s) = Y_1(s) + Y_2(s) \qquad \text{III-13}$$

where

$$Y_1(s) = \frac{N(s)}{1 + G(s)T_K(s)} \qquad \text{III-14}$$

where

$$N(s) = T_K(s)\Big\{ s^{n-1} y_1(t_{K-1}) + s^{n-2}\left[y_2(t_{K-1}) + a_{Kn-1} y_1(t_{K-1})\right] + \ldots + \left[y_n(t_{K-1}) + \cdots + a_{K1} y_1(t_{K-1})\right]\Big\}$$

and

$$Y_2(s) = \frac{R_K(s)G(s)T_K(s)}{1 + G(s)T_K(s)} \qquad \text{III-15}$$

Here the notation $T_K(s)$ is in agreement with III-16.

$$T_K(s) = 1/D(s)$$

$$= \frac{1}{s^n + a_{Kn-1}s^{n-1} + \ldots + a_{K1}s + a_{K0}} \qquad \text{III-16}$$

The denominators of both III-14 and III-15 have a common polynomial factor and the characteristic roots may be found from

$$1 + G(s)T_K(s) = 0 \qquad \text{III-17}$$

or

$$D_1(s)D(s) + K_1N_1(s) = 0. \qquad \text{III-18}$$

The product $D_1(s)D(s)$ of equation III-18 will in general be of greater degree than $N_1(s)$ and hence the degree of the polynomial denominator of $Y_1(s)$ (equation III-14) and $Y_2(s)$ (equation III-15) will be determined as the sum of the number of poles of the compensating block, G(s), and the number of poles of $T_K(s)$.

Similar consideration of the system of Figure 14 with $t = u + t_{K-1}$ within the Kth subinterval yields a solution for Y(s) as

$$Y(s) = Y_1(s) + Y_2(s) \qquad \text{III-19}$$

where

$$Y_1(s) = \frac{N(s)}{1 + H(s)T_K(s)} \qquad \text{III-20}$$

where

$$N(s) = T_K(s)\left\{s^{n-1}y_1(t_{K-1}) + s^{n-2}\left[y_2(t_{K-1}) + a_{Kn-1}y_1(t_{K-1})\right] + \ldots \right.$$

$$\left. \ldots + \left[y_n(t_{K-1}) + a_{Kn-1}y_{n-1}(t_{K-1}) + \ldots + a_{K1}\,y_1(t_{K-1})\right]\right\}$$

and

$$Y_2(s) = \frac{R_K(s)T_K(s)}{1 + H(s)T_K(s)} \qquad \text{III-21}$$

with

$$R_K(s) = \int_{u=0}^{\infty} r(u + t_{K-1})\, e^{us}\, du - \Big\{ s^{p-1} f_1(t_{K-1}) + s^{p-2}\Big[f_2(t_{K-1}) + d_{p-1} f_1(t_{K-1})\Big] + \ldots + \Big[f_p(t_{K-1}) + d_{p-1} f_{p-1}(t_{K-1}) + \ldots + d_1 f_1(t_{K-1})\Big]\Big\}\, H(s). \qquad \text{III-22}$$

Again denominators of both $Y_1(s)$ and $Y_2(s)$ have common polynomial factors and the characteristic roots may be found from

$$1 + H(s)T_K(s) = 0 \qquad \text{III-23}$$

or

$$D_2(s)D(s) + K_2N_2(s) = 0. \qquad \text{III-24}$$

Through the use of block diagram algebra it is possible to make the following important observations. Forward transmission or feedback path compensation of a nonlinear category I or II system results in a category II system described by an equation of the form of II-1. The order of this nonlinear equation depends upon the sum of the number of poles of the incrementally linearized function, $T_K(s)$, and the number of poles of the linear compensating transfer function. For forward transmission compensation the driving function is obtained from $\mathcal{L}^{-1}\{R_K(s)\}$ and for feedback path compensation the driving function is $\mathcal{L}^{-1}\{R_K(s)D_2(s)\}$.

CHAPTER IV

RESPONSE OF AUTONOMOUS SYSTEMS

The system on n linear first order equations upon which the sequential solution is based are said to be autonomous when the functions $\underline{H}_K$ of II-19 are time-independent or stationary. These equations take on the form

$$\frac{d\underline{y}_K}{dt} = \underline{H}_K(\underline{y}_K) \qquad \text{for } t_{K-1} \leq t \leq t_K. \qquad \text{IV-1}$$

The corresponding constant coefficient linear ordinary differential equation is

$$\frac{d^n y}{dt^n} + a_{Kn-1}\frac{d^{n-1} y}{dt^2} + \ldots + a_{K1}\frac{dy}{dt} + a_{K0}y = 0, \qquad \text{IV-2}$$

and the solution, y(t), is simply dependent upon initial conditions of the Kth subinterval. The solution of equation IV-2 is well known and it is both interesting and instructive to use this information for describing the response of the nonlinear systems.

It has already been demonstrated that the sequential solution converges uniformly to the solution, x, of equations with canonical form as shown by II-1. If, in fact, every possible type of linearized solution is investigated, then the component parts of the sequential solution are wholly determined and as a result the solution of the nonlinear system is well characterized.

Figure 15 illustrates a number of possible root ensemble branch locations. Some or all of these may represent branches from which roots are to be selected for establishing the sequential solution of a nonlinear system. In any event the total sequential solution within any subinterval may be considered as the sum of the individual solutions associated with each branch (from Heaviside's partial fraction expansion) provided that this sum satisfies the appropriate initial conditions and remains within the region of existence of the nonlinear equation.

The branch labeled "A" in Figure 15 is representative of all branches of root ensembles which occur on the real axis totally in the left half of the s-plane. The orientation of the arrow has been selected arbitrarily and does not alter the type of autonomous system time response associated with this branch. This response has the form

$$Y_A(t) = K_A e^{-at} \quad \text{where } a > 0. \qquad \text{IV-3}$$

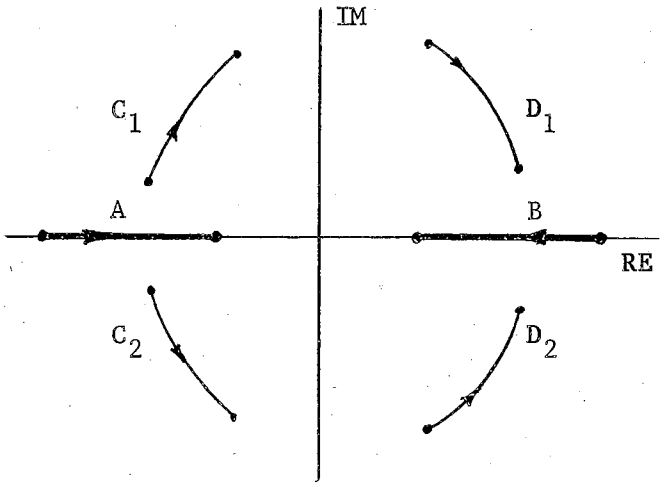

Figure 15. Some Possible Root Ensemble Branch Locations

Within any particular subinterval the constants K_A and a are determined by the initial conditions of that interval. It is apparent, however, that for finite values of K_A the solution $y_A(t)$ tends to zero for large t. It may, therefore, be concluded that if a nonlinear system is operating within the region of existence of its mathematical model and has a branch of its root ensemble wholly on the negative real axis, then there is a term in the sequential solution that tends to zero with large t.

The branch labeled "B" in Figure 15 is intended to represent all branches of root ensembles which occur on the real axis totally in the right half of the s- plane. Again the arrow orientation is meaningless when considering the form of the associated time response. The form of the response corresponding to this branch is

$$y_B(t) = K_B\, e^{bt} \quad \text{where } b>0. \qquad \text{IV-4}$$

For any subinterval the constants K_B and b are determined by the initial conditions of that interval. Except for the trivial case where $K_B = 0$ for all subintervals it is evident that $|y_B(t)|$ becomes arbitrarily large for large t. The presence of a term such as that of equation IV-4 in the sequential solution leads to the overall solution magnitude becoming exceedingly large and eventually of sufficient size to exceed the allowable output.

Branches "C_1" and "C_2" are complex conjugate. Each is in the left half of the s-plane and each has a time response within any subinterval that can be expressed as an exponential. By virtue of the complex conjugate nature of these root ensemble branches it is convenient to

combine these time functions into

$$y_C(t) = K_C e^{-ct} \sin(wt + \phi), \text{ where } c, w > 0. \qquad \text{IV-5}$$

Although the parameters K_C and c vary from subinterval to subinterval, the function, $y_C(t)$, has a magnitude which tends to zero for large t.

The final pair of complex conjugate branches in Figure 15 are denoted as "D_1" and "D_2". The terms in a sequential solution corresponding to these branches may be combined in a manner similar to that employed for the previous functions. Here the resultant term acquires the form

$$y_D(t) = K_D e^{dt} \sin(wt + \phi), \text{ where } d, w > 0. \qquad \text{IV-6}$$

Equation IV-6 is composed of the product of the increasing relation $K_D e^{dt}$ and the bounded periodic function, $\sin(wt + \phi)$. The resultant product is oscillatory but of arbitrarily large amplitude for increasing t.

In summary it may be said that terms in a sequential solution which are paired with ensemble branches entirely in the left half of the s-plane represent stable portions of the response of a nonlinear system to initial conditions. On the other hand any term in a sequential solution which corresponds to a branch (or complex conjugate branches) totally in the right half of the s-plane represents an unstable portion of the response. From this it follows that any nonlinear control system is stable if it has a root ensemble made up of branches confined to the left half of the plane. If, however, one or more branches are totally in the right half plane the system is unstable.

In Figure 15 each of the branches is shown with an arrow. This is of course in keeping with the convention established in Chapter III. The $y = 0$ point may or may not be located at the extreme tail end of each branch. It is highly possible that the root locations for values of y where $y > 0$ and those for $y < 0$ are not the same. However, it will often be found for physical devices that the root locations depend only upon $|y|$ and not upon the algebraic sign. Under these circumstances the branches of the root ensemble will eminate from a $y = 0$ point at an end of the ensemble branches.

There are several additional root ensemble branch locations depicted in Figure 16. Here the symmetry with regard to $|y|$ is presumed to exist although the conclusions drawn are not necessarily based upon this property. The branches of this figure all cross the imaginary axis from one half plane to the other. The arrow orientations become extremely important when considering these configurations. The complex conjugate branches labeled "E_1" and "E_2" indicate that for small $|y|$ the form of the subinterval solution is

$$y_E(t) = K_E e^{\alpha t} \sin(wt + \phi), \text{ where } \alpha > 0. \qquad \text{IV-7}$$

For larger values of $|y|$ the subinterval response is

$$y_E(t) = K_E e^{-\alpha t} \sin(wt + \phi), \text{ where } \alpha > 0. \qquad \text{IV-8}$$

If for any particular system the initial conditions at $t = t_0$ are such that the sequential solution roots are on portions of the ensemble branches, E, in the right half of the plane then the corresponding solution is of an oscillatory nature but with growing amplitude. Eventually this results in the total solution amplitude reaching a point

so that the response term corresponding to these branches has the form of IV-8. If all other branches of the root ensemble are in the left half plane, the resultant sequential solution exhibits a "limit cycle". Any initial conditions which cause the solution roots to begin in the left half plane also cause the overall response to diminish until the limit cycle condition is again reached.

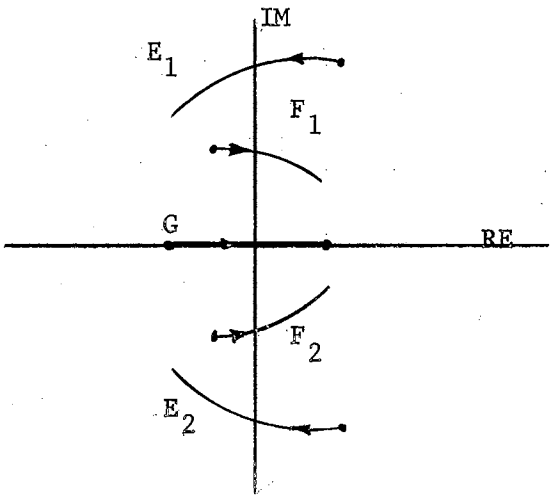

Figure 16. Additional Root Ensemble Branch Locations

The conjugate pair of branches, F, cross the vertical axis from left to right with increasing $|y|$. For small magnitudes the subinterval response corresponding to these branches is of the form

$$y_F(t) = K_F e^{-ft} \sin(wt + \phi), \text{ where } f > 0. \qquad \text{IV-9}$$

For increases in t this term will be oscillatory with decreasing amplitude. Unless some other portion of the sequential solution forces

the total response to become sufficiently great in size so as to necessitate the selection of roots from those segments of the branches in the right plane, it is evident that IV-9 will tend to zero for large t. If by virtue of the initial conditions or some other term in the sequential solution, the roots are selected from the right half plane portion of the F branch, then the corresponding subinterval response is of the form

$$y_F(t) = K_F e^{ft} \sin(wt + \phi), \text{ where } f > 0. \qquad \text{IV-10}$$

In spite of the fact that IV-10 has a divergent amplitude, its oscillatory nature implies that there is the possibility of the total solution diminishing sufficiently to cause the root selection to be made from the left half plane segments of F. If then the amplitude decays sufficiently it may never again assume the form of IV-10. The ensemble branch crossing from left to right does not necessarily imply instability. It will indicate a highly oscillatory response, however, and points strongly toward regions of nonlinear system operation which are unstable. In any case, good design procedures will generally dictate that a system be limited to operation as far removed to the left of the vertical axis as is feasible.

The branch "G" of Figure 16 has a clearly defined point of instability. If for any reason the total sequential solution requires selection of points from this ensemble branch to the right of the origin, then the corresponding time response is unstable. Consider the form of the time response. It is

$$y_G(t) = K_G e^{gt} \text{ where } g > 0. \qquad \text{IV-11}$$

Obviously $y_G(t)$ increases monotonically and adds to the total sequential solution making it arbitrarily large.

Figures 17 through 26 illustrate some of the autonomous system characteristics described in this chapter. Figure 17, itself, depicts a triode oscillator with a tuned grid circuit (see Appendix B) having a symmetric nonlinearity. Mutual coupling between the plate and grid provides feedback so that the mathematical model of this network is

$$\frac{d^2y}{dt^2} - 0.8(1-y^2)\frac{dy}{dt} + y = 0, \qquad \text{IV-12}$$

where y represents a constant multiple of the incremental grid voltage, e_g, in ratio to the saturation voltage, E_s. This saturation voltage is shown in Figure 18 where a plot of incremental grid voltage versus AC plate current illustrates the nonlinearity of the electron tube. Figure 19 is the root ensemble of this circuit and shows the locations of the linearized systems roots from $|y| = 0$ to $|y| = 2$. The vertical axis crossings from right to left half planes is indicative of a limit cycle. Figure 20 illustrates a phase plane plot for three initial conditions and the corresponding time responses are shown in Figure 21 (see Appendix C).

Figures 22 through 26 are associated with a series resistance-inductance network. The inductance is assumed nonlinear and dependent upon the current flow as illustrated by Figure 22. The input is assumed to be the voltage applied to this network and the voltage across the resistor (R = 10 ohms) is taken as the output. The equation relating the input voltage to the current is

$$e_{in} = 10i + f(i)\frac{di}{dt} \qquad \text{IV-13}$$

where

$$f(i) = \begin{cases} 6.293 & |i| > 10/3 \\ 10 - 3i^2 - 0.8i^3 & -10/3 \leq i \leq 0 \\ 10 - 3i^2 + 0.8i^3 & 0 < i \leq 10/3 \end{cases}$$

The solution of IV-13 in conjunction with the auxiliary equation, $e_0 = iR$, provides the input-output relationship. Figure 23 shows the root ensemble and it is interesting to note the overlapping nature of the branch. Figure 24 is the phase plane plot obtained from the sequential solution while Figure 25 shows a time plot for the same initial condition. Equation IV-13 is directly integrable and the solution is shown in Figure 26 for the sake of comparison.

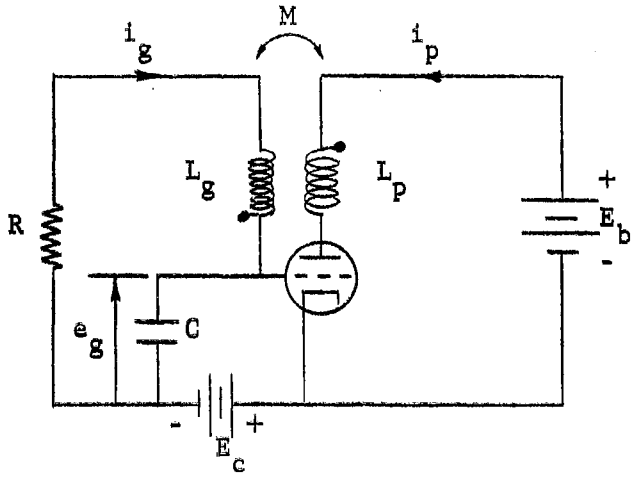

Figure 17. A Triode Oscillator with Tuned Grid Circuit and Mutual Coupling

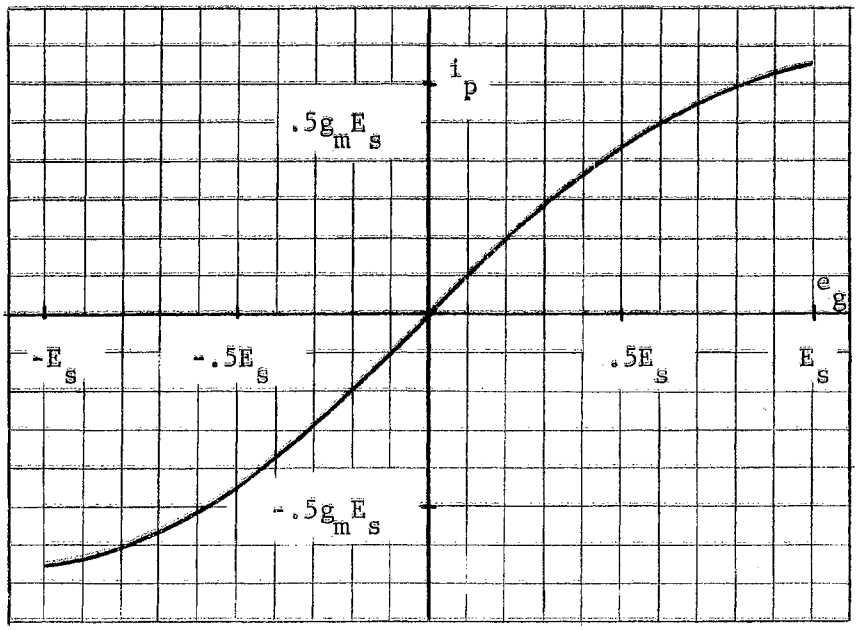

Figure 18. Incremental Plate Current-AC Grid Voltage Characteristic

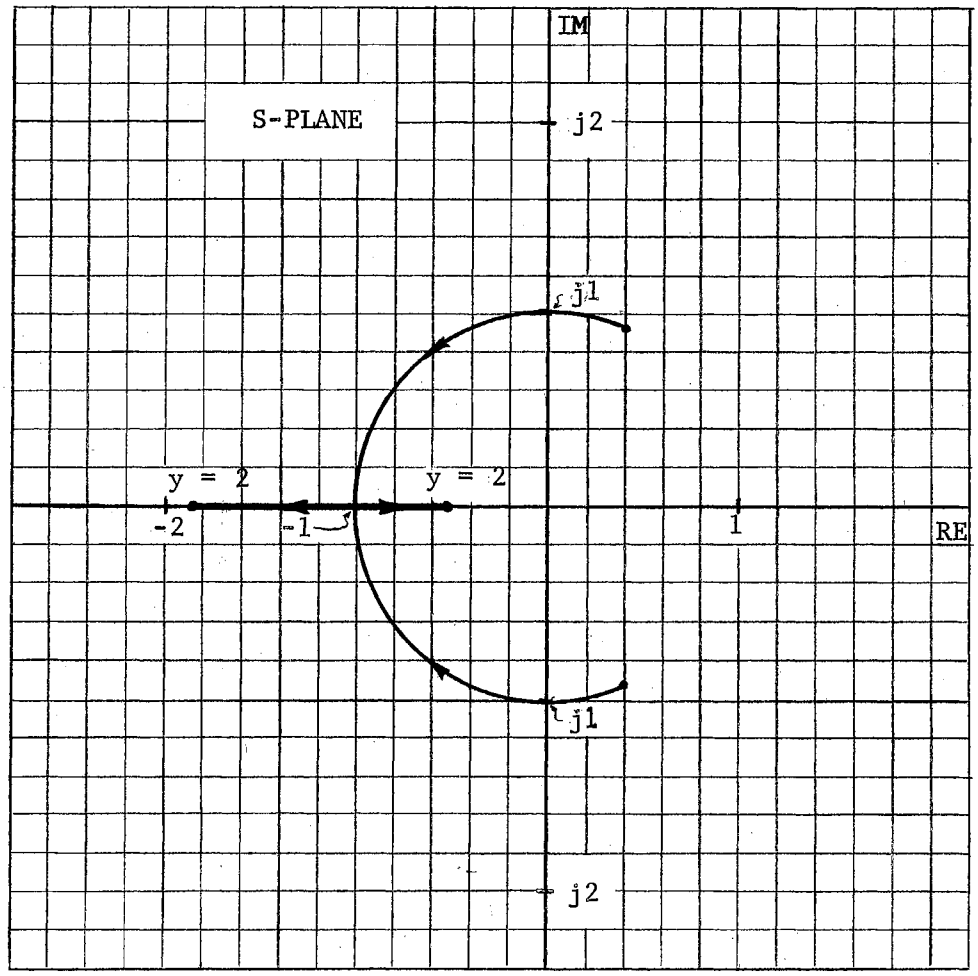

Figure 19. Root Ensemble for the Oscillator

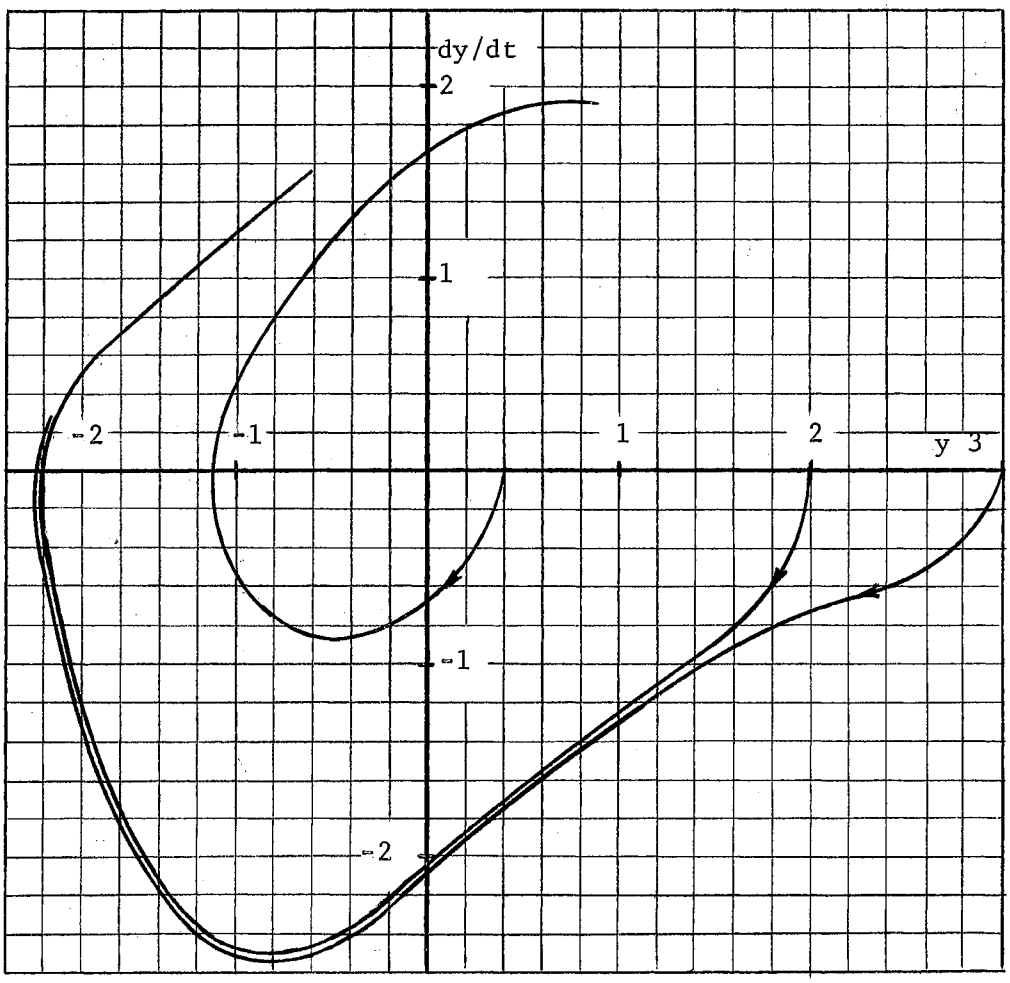

Figure 20. Phase Plane Plot for Nonlinear Oscillator

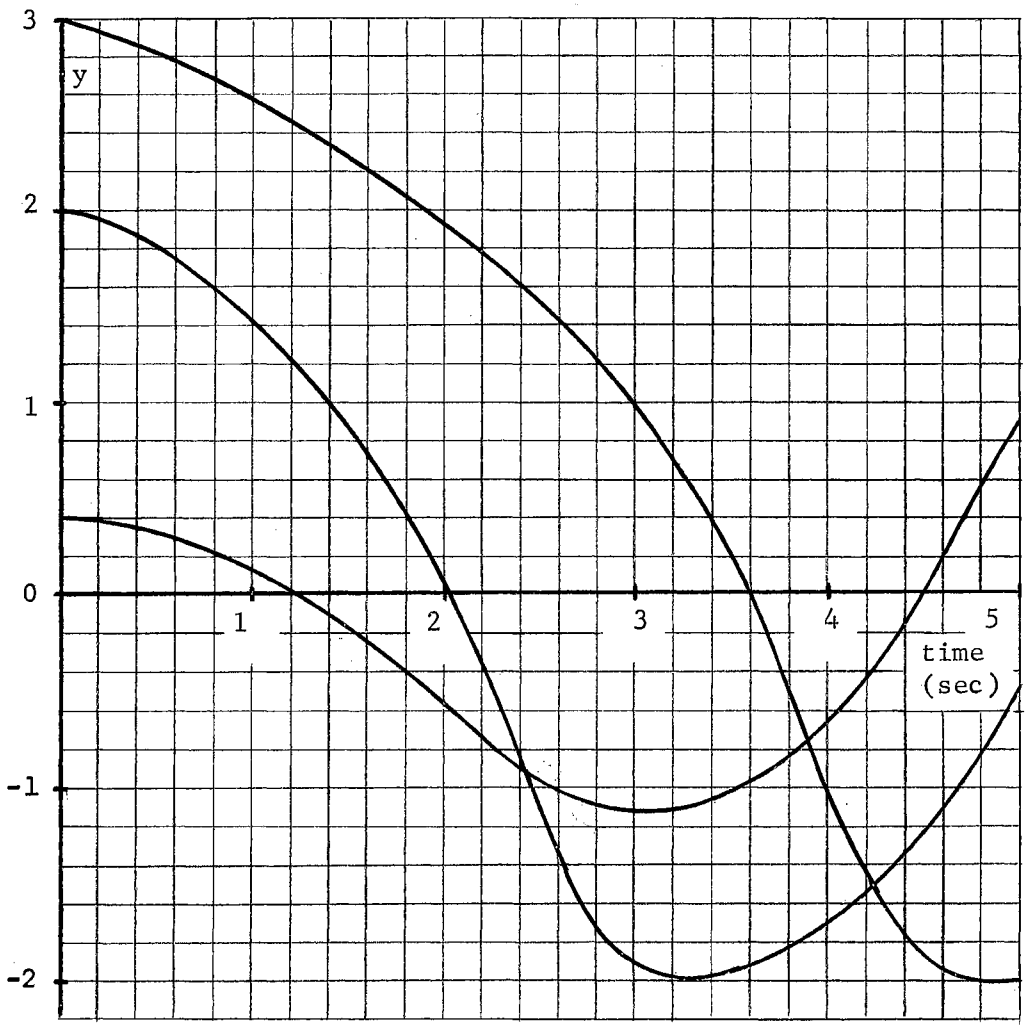

Figure 21. Nonlinear Oscillator Time Response to Initial Conditions

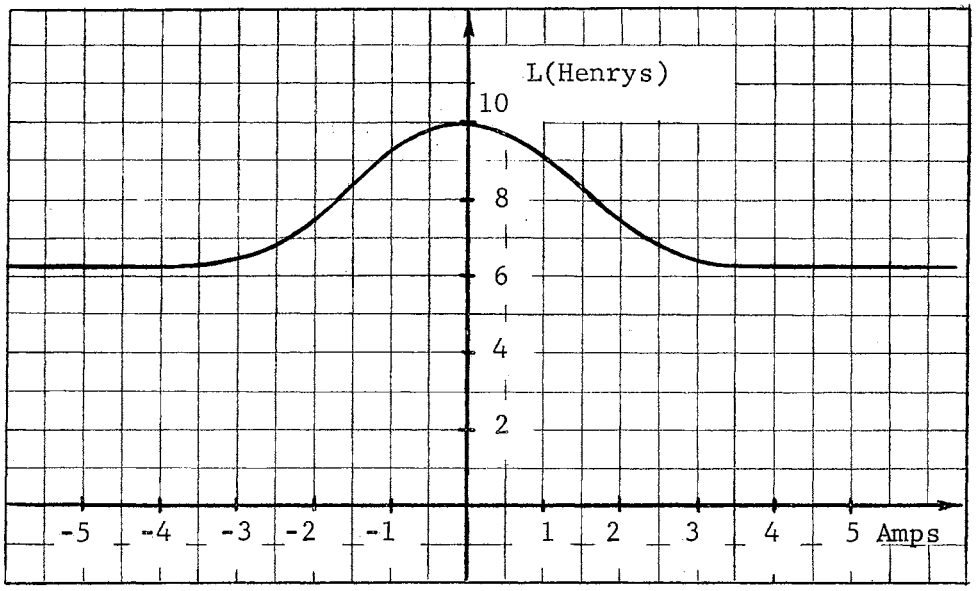

Figure 22. Variation of Inductance with Current

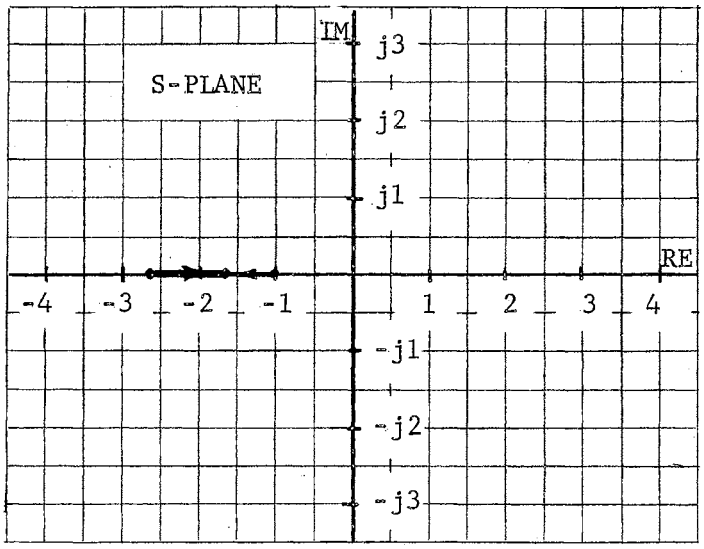

Figure 23. Root Ensemble for Resistor-Nonlinear Inductor Network

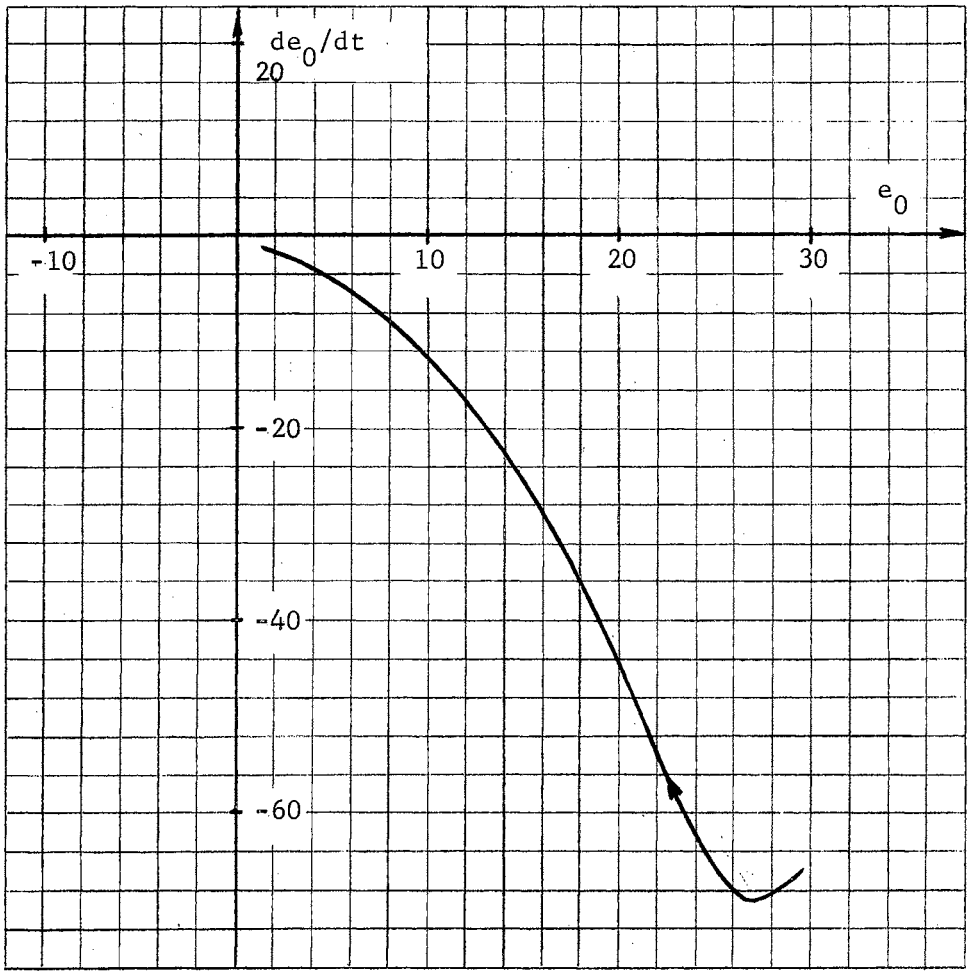

Figure 24. Phase Plane Plot for Nonlinear Inductance-Resistance Network

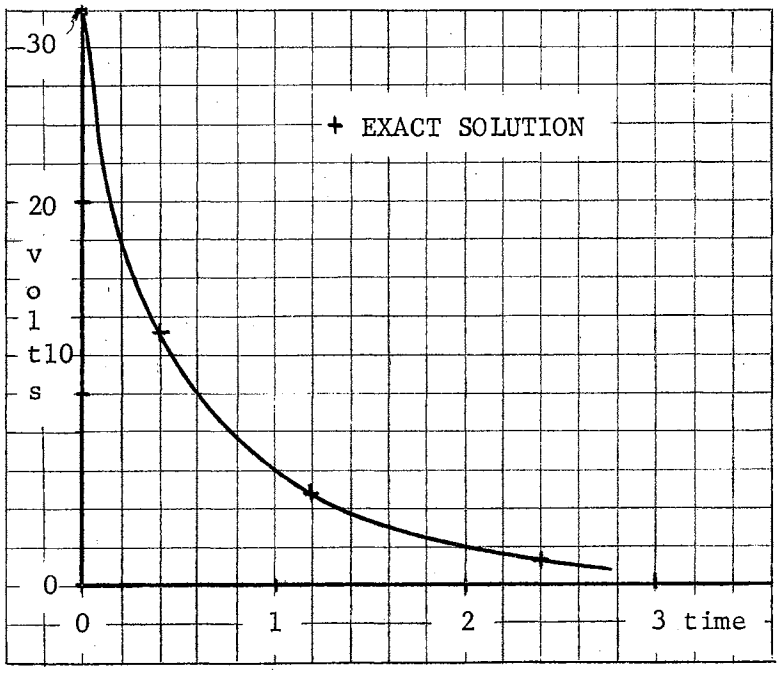

Figure 25. Sequential Solution Versus Time

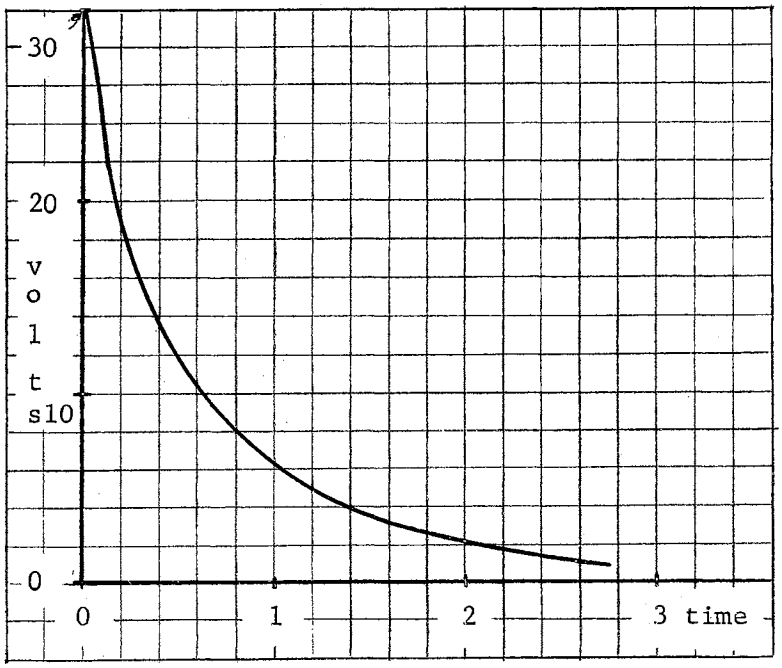

Figure 26. Actual Solution of Nonlinear Network

CHAPTER V

THE LOCUS OF THE ROOT ENSEMBLE

The block diagram manipulations of Chapter III have indicated a scheme of compensation based upon the closed loop operation of category I or II systems. From this investigation it was discovered that within each of the subintervals $\left[t_{j-1}, t_j\right]$ the nonlinear system's sequential solution is characterized by the denominator polynomial

$$1 + P(s) \qquad \text{V-1}$$

where P(s) can be written as

$$P(s) = G(s)T_j(s) \qquad \text{V-2}$$

for forward transmission compensation while for feedback path compensation it is

$$P(s) = H(s)T_j(s). \qquad \text{V-3}$$

The quantity, P(s), in linear analysis is known as the open-loop transfer function and it will be convenient to continue this designation. The characteristic polynomial of V-1 may have either a forward transfer function of the form of V-2 or V-3 without materially altering the type of closed loop response. As a result it is possible to combine the procedures for characterizing the responses while reserving an enumeration of the slight differences until later. To accomplish this P(s) will be

assumed of the form of V-2. One change in nomenclature results in considerable additional convenience. Henceforth G(s) will be replaced by KG'(s). The characteristic equation then becomes

$$1 + KG'(s)T_j(s) = 0 \qquad \text{V-4}$$

and is written explicitly in terms of the static loop sensitivity, K.

Consideration of V-4 under the circumstances that G'(s) and $T_j(s)$ are rational functions of s as outlined in Chapter III leads to V-5 as an alternate form of V-4 where D(s) is the denominator polynomial of $T_j(s)$,

$$D(s)D_1(s) + KN_1(s) = 0 \qquad \text{V-5}$$

$D_1(s)$ is the denominator polynomial of G'(s) and $N_1(s)$ represents the numerator polynomial of G'(s). The product $D(s)D_1(s)$ is also assumed to be of greater degree than the polynomial $N_1(s)$ and hence the degree of V-5 is established by this product. There are then as many characteristic roots as the degree of the product of D(s) (degree n) and $D_1(s)$ (degree v). Since for every integer value of j such that $1 \leq j \leq m$ the functions $T_j(s)$ have denominators with fixed degree, the products $D(s)D_1(s)$ which result will have exactly the same number of roots. If now K is allowed to assume values such that $K > 0$, there are n + v roots of the characteristic equation in the jth subinterval for each K. Each of these roots appears on a constant gain, K, branch of a root ensemble from which m roots (not necessarily distinct) are to be selected for the sequential solution. An illustration of the variation of the root ensemble with K on the s-plane will be called a locus of the root ensemble or more concisely an ensemble locus.

Equation V-4 will be used to establish some of the properties of the ensemble locus. The problem is simply that as K varies, values of s must be obtained which satisfy

$$KG'(s)T_j(s) = -1. \qquad \text{V-6}$$

Equation V-6 is generally encountered in linear system theory whereupon it is decomposed into the well known magnitude and angle conditions. In terms of present functions this may be accomplished by replacing the left side of V-6 with its polar equivalent.

$$KG'(s)T_j(s) = Fe^{j\beta}. \qquad \text{V-7}$$

The right side of V-6 may be rewritten in its polar form as

$$-1 = e^{j(1 + 2z)\pi} \text{ where } z = 0, \pm 1, \pm 2 \ldots \qquad \text{V-8}$$

so that V-6 has the polar form

$$Fe^{j\beta} = 1e^{j(1 + 2z)\pi}. \qquad \text{V-9}$$

From V-9 the magnitude condition is

$$\left|KG'(s)T_j(s)\right| = F = 1 \qquad \text{V-10}$$

and the angle condition is

$$\angle KG'(s)T_j(s) = \beta = (1 + 2z)\pi \text{ where } z = 0, \pm 1, \pm 2, \ldots \qquad \text{V-11}$$

From V-10 and V-11 it is observed that roots which correspond to the same value of y on the ensemble can be treated in the conventional root locus manner. After several typical root loci are plotted adjacent points representing the same gain may be connected. The result is a

branch of the closed loop system root ensemble.

Some of the interesting features of the ensemble locus are easily traced through the application of root locus rules to corresponding y roots on the ensemble. These closed loop ensemble properties lend themselves readily to system analysis and synthesis.

Properties of the Ensemble Locus

The following is a listing of some of the pertinent ensemble locus properties.

1.) The number of branches of the ensemble locus is exactly equal to the order, n, of the nonlinear system equation (either category I or II) and the number of poles, v, of the linear compensating device.

2.) The locus of the closed loop ensemble branches for increasing values of the static sensitivity, K, begins at the open loop ensemble branches and ends at an open loop zero or infinity. Linear system poles in the open loop case represent degenerate branches of the ensemble having nondistinct root locations. The zeros of the open loop system are fixed in location and are attributed to the linear device only.

3.) A point on the real axis is a point on the ensemble locus if the number of zeros and branches (or branch segments) to the right of that point is odd.

4.) Each point of an ensemble branch approaching infinity for large values of K does so along an asymptote with angle

$$\gamma = \frac{(1 + 2k)180^{0}}{n + v - w}, \quad k = 0, \pm 1, \pm 2, \ldots \qquad V\text{-}12$$

where n is the order of the original nonlinear system equation, v is

the number of poles and w the number of zeros of the compensating device.

5.) The real axis intercept point, σ_0, for each of the asymptotes previously described is determined from

$$\sigma_0 = \frac{\sum_{c=1}^{n+v} (P_c) - \sum_{d=1}^{w} (z_d)}{n + v - w} . \qquad \text{V-13}$$

The summation, $\sum_{c=1}^{n+v} (P_c)$, represents the sum of the poles from the open loop root ensemble branches corresponding to the same y as the one of interest on the closed loop ensemble. The sum, $\sum_{d=1}^{w} (z_d)$, is the sum of the open loop zeros and n, v, and w are as indicated in property 4.

Properties 4 and 5 indicate that as an ensemble branch moves toward infinity for large gain values the points on each ensemble branch approach parallel asymptotes. The angle of these asymptotes is calculated from 4 while 5 determines the real axis crossing points.

Figures 27, 28, and 29 illustrate the locus principles as applied to typical third, second, and first order nonlinear systems respectively. The compensating device is restricted to an adjustable gain only. Figure 27 is the ensemble locus made possible by placing a feedback path around the system of Figure 5. With increasing gain the complex conjugate branches of the ensemble move into the right half plane and reveal an instability at moderate values of K. There are no zeros and so the ensemble branches must approach asymptotes with angles given by

$$\gamma = (1 + 2k)60^{\circ} \text{ for } k = 0, 1, 2. \qquad \text{V-14}$$

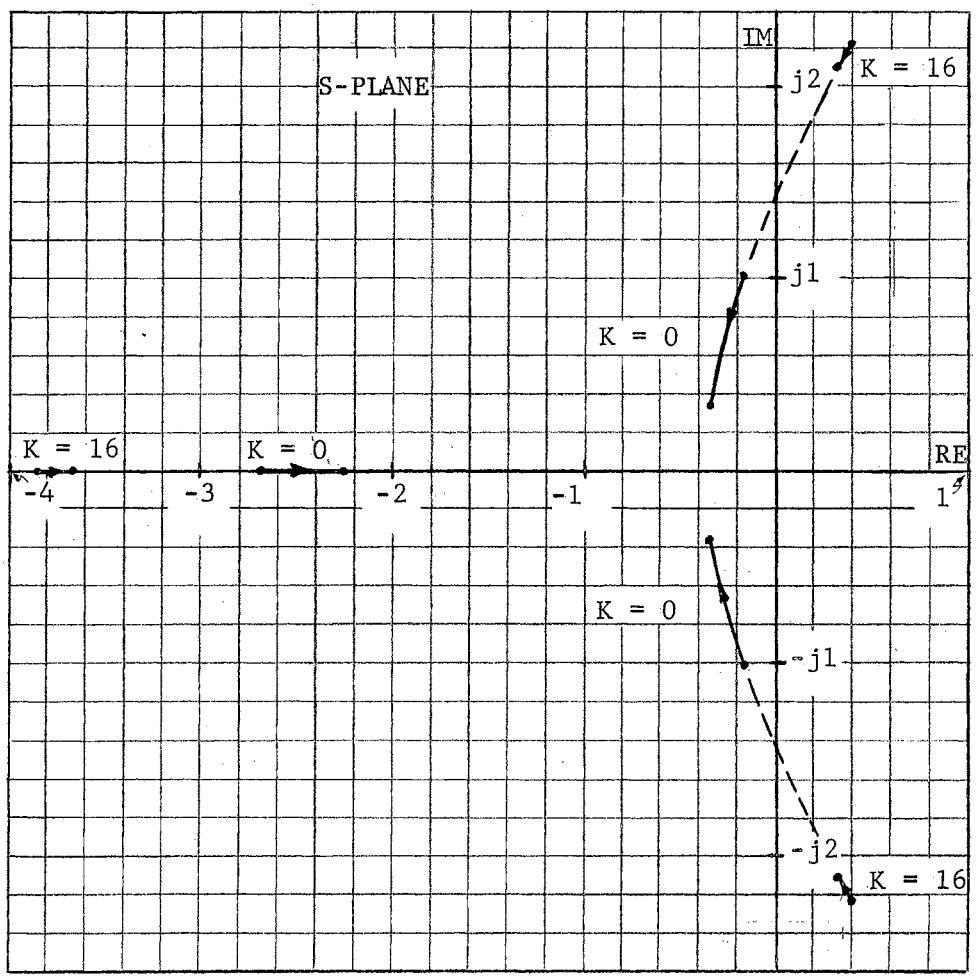

Figure 27. Ensemble Locus for a Third Order System

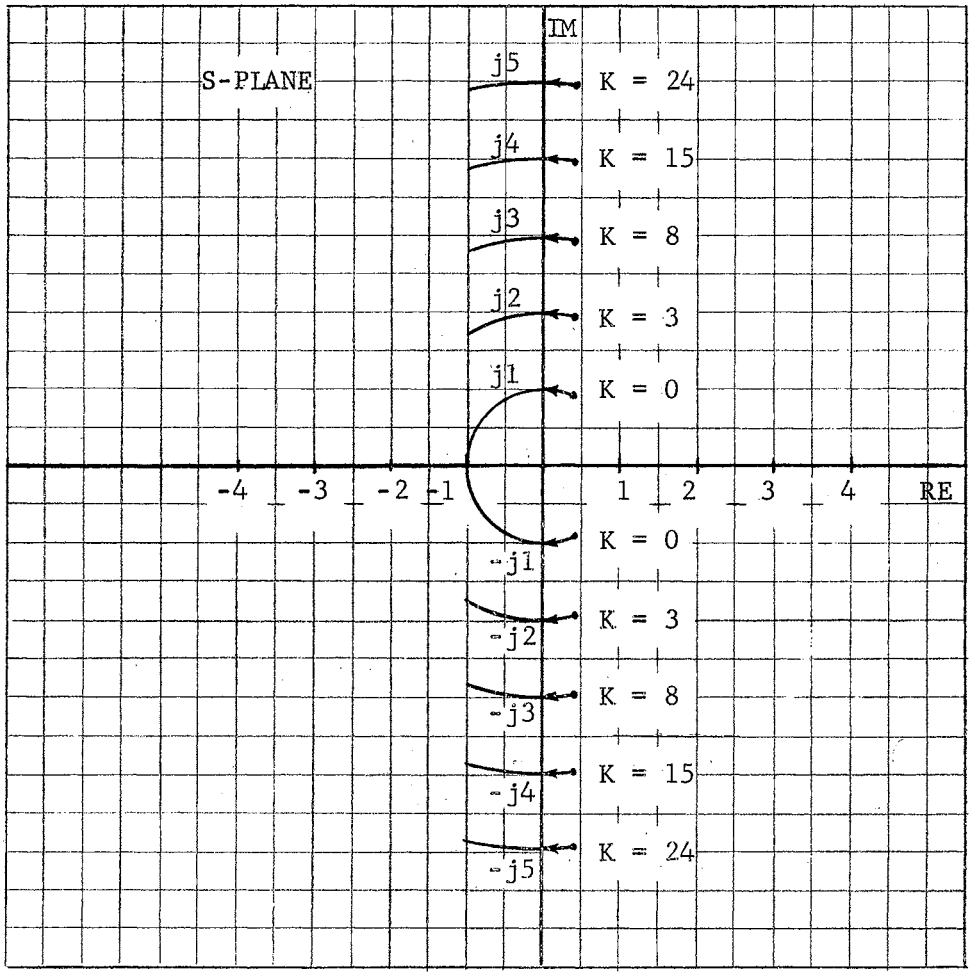

Figure 28. Root Ensemble Locus for Second Order System with a Limit Cycle

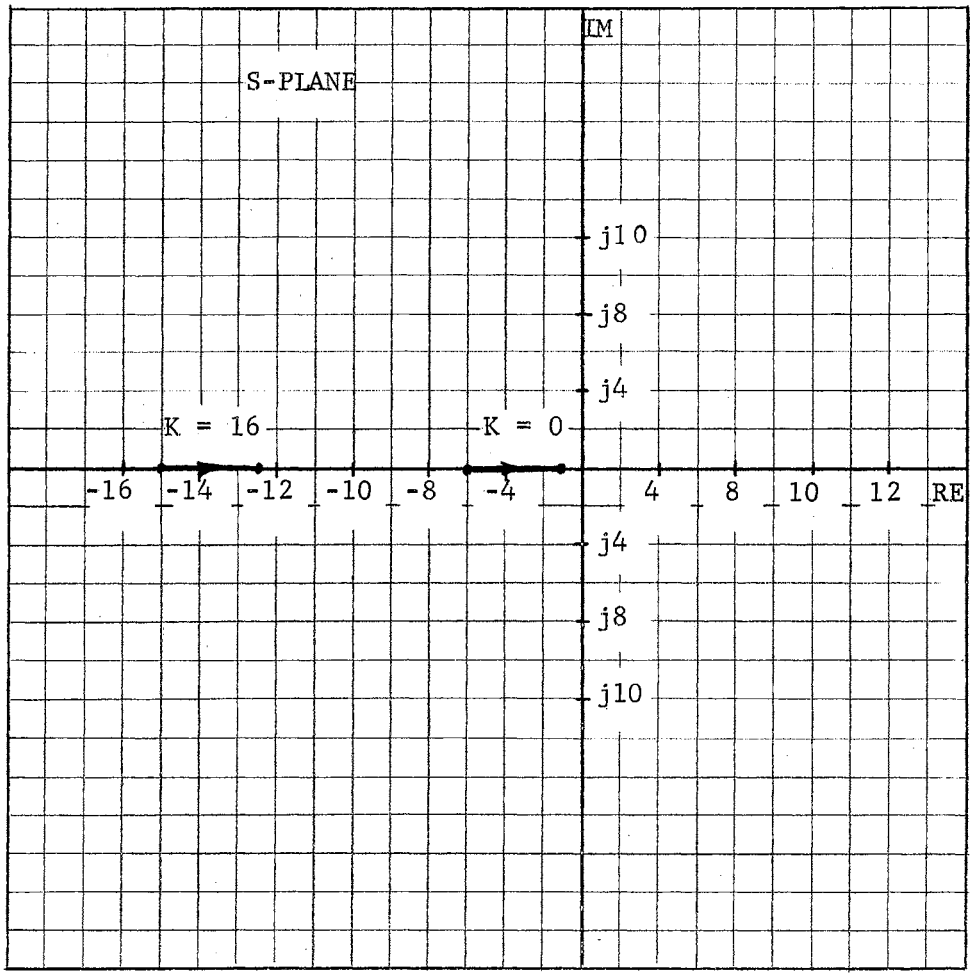

Figure 29. Ensemble Locus of Motor Speed Control System

In each case the corresponding y-value poles have a summation,

$$\sum_{c=1}^{n+v} (P_c) = 3 \qquad \text{V-15}$$

while

$$\sum_{d=1}^{w} (z_d) = 0. \qquad \text{V-16}$$

From V-15 and V-16 it is apparent that every asymptote associated with an ensemble branch intersects the real axis at $\sigma_o = -1$.

Figure 28 is the ensemble locus of a system having a plant which exhibits a limit cycle. Branch locations are altered only in the vertical direction and so the corresponding category II system also displays a limit cycle characteristic.

Figure 29 is the ensemble locus of the motor speed control system of Figure 8. The single ensemble branch moves along the negative real axis for increasing K. In so doing it maintains its length and represents closed loop time constants of decreasing magnitude.

The ensemble locus shows the locations of the roots to be selected for use in the sequential solution of the nonlinear closed loop system. There are certain differences between feedback path compensation and forward transmission compensation, however. These differences exist only with regard to the numerator terms of equations III-14, III-15, III-20, and III-21. Thus the transform of the output, Y(s), is in each of these arrangements characterized by the same type of ensemble branches but the sequential selection of roots is effected by the difference in numerators.

Shaping the Ensemble Locus

It is often desired to produce certain response characteristics. The ensemble locus is well suited for not only the determination of the response but also for its shaping through alterations in ensemble branch locations. This is usually accomplished by the introduction of poles and zeros. Each additional pole adds a branch to the closed loop system ensemble and increases the difficulty of calculating the time response.

The effects of compensating pole and zero locations are essentially the same as encountered in the linear system case. Added zeros to the left of the plot tend to bend the locus to the left while poles added to the left have the opposite effect. As an illustration of an adjustment scheme, a zero has been introduced into the open loop root ensemble plot of the third order system of Figure 27. The result is shown in Figure 30. The branches which previously had crossed the vertical axis into the right half plane now remain entirely within the left half plane. The system has been compensated for the instability which it had exhibited.

This has not been intended as a discourse on the methods and reasons for the need of compensation. Instead, it has been meant to show the complete carry-over of the techniques of linear system theory to the synthesis of feedback systems having nonlinear plants described by equations of the form of II-1.

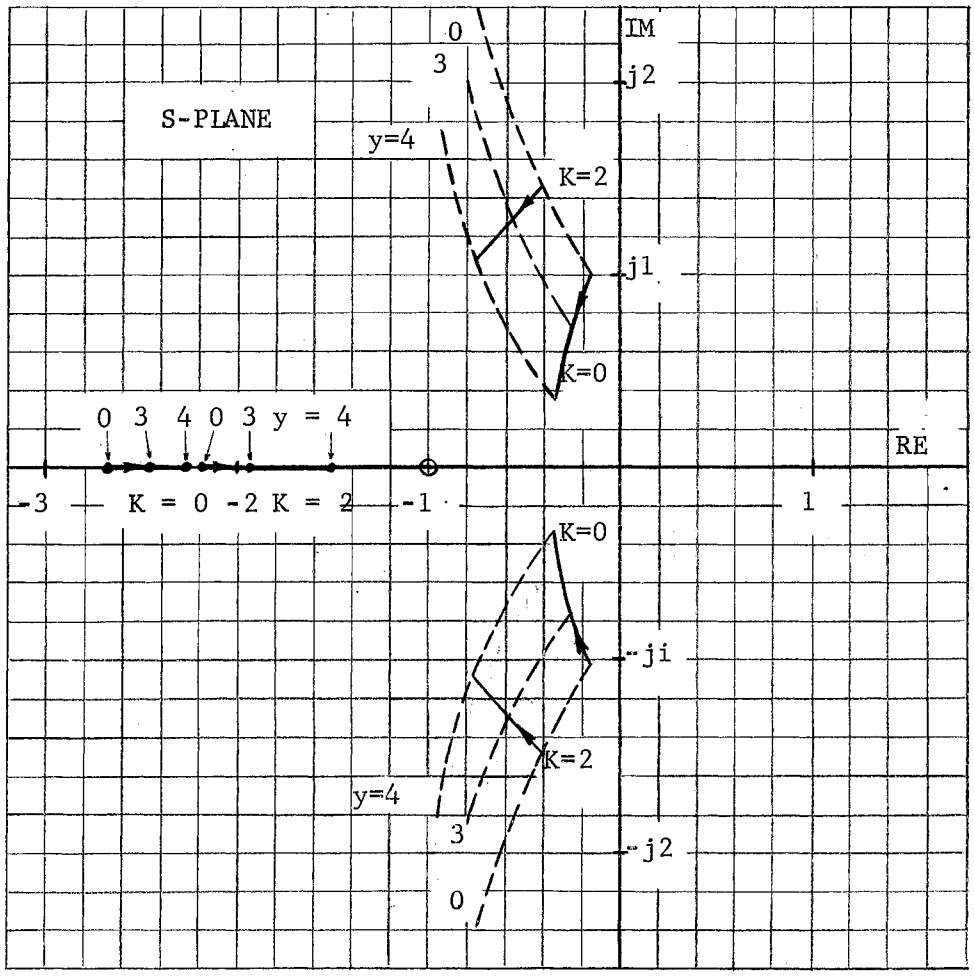

Figure 30. Root Ensemble of Nonlinear System Compensated by a Zero at -1

CHAPTER VI

SUMMARY AND CONCLUSIONS

A method has been achieved for linearizing the mathematical model of certain control systems described by equations of the form

$$\frac{d^n x}{dt^n} + f_{n-1}(x)\frac{d^{n-1}x}{dt^{n-1}} + \ldots + f_1(x)\frac{dx}{dt} + f_0(x)\, x = F(t) \qquad \text{VI-1}$$

with initial conditions at $t = t_0$ of

$$x = x_{10};\ \frac{dx}{dt} = x_{20};\ \ldots;\ \frac{d^{n-1}x}{dt^{n-1}} = x_{n0} \qquad \text{VI-2}$$

where the functions $f_{n-1}(x)$, $f_{n-2}(x)$, ..., $f_0(x)$ and $F(t)$ are all of class C^1 in some region, R. The approximate solution, y, is developed around a property of differential equations which physical scientists and engineers have utilized to considerable advantage for some time. In a manner of speaking, this property indicates that the solution of a differential equation depends continuously upon the differential equation for given initial values.

The function, y, has been designated the sequential solution and approximates the solution, x, to the desired degree of accuracy. The maximum error in the sequential solution on the interval $0,T$ has been shown to have a value such that

$$\left| \underline{x} - \underline{y} \right| < \triangle e^{2LT}/L \qquad \text{VI-3}$$

where Δ depends inversely upon the number, m, of subintervals of the partition, P_m, of $[0,T]$. It was concluded that y and the first (n-1)th derivatives of y are continuous functions defined on this interval in a manner as to converge uniformly to x and its first (n-1)th derivatives with increases in the number of subintervals.

Considerable importance has been placed upon operational methods made available through the use of the linearized system. A block diagram representation of the nonlinear system was made possible through the transformation of the analysis into the frequency domain. In spite of the fact that actual response computations are quite lengthy when using this representation, the block diagram proves to be of value from a conceptual standpoint in both analysis and synthesis.

Reference is made to the root ensemble throughout this thesis. The ensemble is an important consequence of the block diagram representation and is an aggregate of all the characteristic roots belonging to the linearized system's transfer functions. The ensemble is constructed without knowledge of the solution of the nonlinear equation, but requires that the region of definition of the solution be well defined. The root ensemble is itself time independent and describes the nonlinear system for both forced and autonomous responses.

Close examination of closed loop control systems reveals two natural divisions. The first of these (category I) is characterized by a closed loop equation of the form of II-1. The second case (category II) is that in which the forward transmission is governed by this same relationship.

Characterization of the response of autonomous systems is greatly facilitated through the use of the root ensemble. Here it has been

demonstrated that:

1.) branches of the ensemble which lie wholly in the left half plane represent stable terms in the total solution,

2.) branches of the ensemble which are totally confined to the right half of the s-plane represent unstable terms in the total solution and consequentially the total solution is unstable,

3.) complex conjugate branches which cross the vertical axis from right to left with increasing solution magnitudes characterize a limit cycle if all other branches are confined to the left half plane,

4.) complex conjugate branches which cross the vertical axis from left to right represent highly oscillatory and perhaps even unstable solution terms, and finally

5.) a branch on the axis of reals which crosses the vertical axis from left to right leads to an unstable term in the total solution for values of y causing the root selection to be made to the right of the origin.

Further use is made of the root ensemble for category II systems by first demonstrating that these have characteristic roots which are related to the root ensemble branches in the same manner that the open and closed loop poles of a linear system are connected. In view of this, rules for constructing ensemble branch loci are presented with indications of possible methods of compensation.

The nonlinear systems theory presented herein has been based upon the use of the sequential solution and associated operational methods. Although this tool has proven valuable in the investigation of nonlinear systems there are some notable omissions in its description. Among these is the solution of nonlinear systems (both category I and

II) in the presence of forcing functions. Of particular interest are the cases in which the driving functions are sinusoids, steps, and ramps. Root ensemble characterization of such nonlinear phenomena as jump resonance, entrainment as well as frequency multiplication and demultiplication are believed by the author to be a possibility. These investigations are undoubtedly subjects for continued research.

SELECTED BIBLIOGRAPHY

1. Thaler, George J. and Marvin P. Pastel. Analysis and Design of Nonlinear Feedback Control Systems. New York: McGraw-Hill Company, Inc., 1962, pp. 334-359.

2. Levine, Leon. Methods for Solving Engineering Problems Using Analog Computers. New York: McGraw-Hill Book Company, Inc., 1964.

3. Gibson, John E. Nonlinear Automatic Control. New York: McGraw-Hill Book Company, Inc., 1963, pp. 342-438.

4. Struble, Raimond A. Nonlinear Differential Equations. New York: McGraw-Hill Book Company, Inc., 1962.

5. Birkhoff, Garett and Gian-Carlo Rota. Ordinary Differential Equations. Boston: Gin and Company, 1962.

6. Ince, E. L. Ordinary Differential Equations. New York: Dover Publications, Inc. Dover Edition, 1956.

7. McLachlan, N. W. Ordinary Nonlinear Differential Equations in Engineering and Physical Sciences. London: Oxford University Press, Second Edition, 1958.

8. Chestnut, Harold and Robert W. Mayer. Servomechanisms and Regulating System Design, Vol. I. New York: John Wiley and Sons, 1959.

9. Koepsel, Wellington W. "Jump Resonance in a Third Order Nonlinear Control System", Doctorial Dissertation Oklahoma State University, May 1960.

10. Apostol, Tom M. Mathematical Analysis. Reading: Addison-Wesley Publishing Company, Inc.

APPENDIXES

APPENDIX A

DETERMINATION OF THE MATHEMATICAL MODEL OF TYPICAL NONLINEAR SYSTEMS

The root ensembles of Figures 4, 7, and 10 are a direct result of the mathematical models used to describe the associated nonlinear systems. These models are investigated and their root ensembles determined.

The Closed Loop Positional Control System with Saturating Amplifier

The mathematical model of this system (see Figure 2) is achieved from two essential relationships. This first is a consequence of the summing device and may be written as

$$r - c = e_1 \qquad \text{A-1}$$

while in terms of the transform variable s the second is

$$C(s) = E_2(s) \cdot \frac{K_M}{s(\tau_M s+1)} \qquad \text{A-2}$$

Substitution of equation A-2 into A-1 leads to

$$R(s)(s\tau_M + 1)s - K_M E_2(s) = E_1(s)\, s(\tau_M s+1) \qquad \text{A-3}$$

Now if this system is restricted to have zero input, the corresponding mathematical model is the differential equation

$$\tau_M \frac{d^2 e_1}{dt^2} + \frac{de_1}{dt} + K_M e_2 = 0. \qquad \text{A-4}$$

The output, e_2, of the saturating amplifier is related to the

input by the equation

$$e_2 = (a - be_1^2)e_1 \qquad \text{A-5}$$

and substitution into A-4 yields

$$\frac{d^2e_1}{dt^2} + \frac{1}{\tau_M}\frac{de_1}{dt} + \frac{K_M}{\tau_M}(a - be_1^2)e_1 = 0. \qquad \text{A-6}$$

This equation has the form of II-1 and the linearized equation will be

$$\frac{d^2e_1}{dt^2} + a_1\frac{de_1}{dt} + a_0e_1 = 0, \qquad \text{A-7}$$

within each of the subintervals. The characteristic roots of A-7 are calculated from

$$s = a_1/2 \pm 1/2\sqrt{a_1^2 - 4a_0}. \qquad \text{A-8}$$

If these roots are plotted for all possible values of a_1 and a_0 the result is the root ensemble. Since a_1 is a constant given by

$$a_1 = 1/\tau_M \qquad \text{A-9}$$

the only variation in root location is due to a_0. For the ensemble of Figure 4 values of y have been selected such that

$$4a_0 > a_1^2 \qquad \text{A-10}$$

with a = 1, b = 0.5, and $\tau_M = 0.5$.

The Third Order System with Nonlinear Feedback Element

In accordance with the block diagram configuration the system of Figure 5 has the relationships

$$r - h(y) = e \qquad \text{A-11}$$

and

$$\frac{Y(s)}{E(s)} = \frac{K}{s(T_1 s+1)(T_2 s+1)} \; . \qquad \text{A-12}$$

Equation A-12 may be rewritten as

$$Y(s) \cdot s(T_1 s+1)(T_2 s+1) = KE(s) \qquad \text{A-13}$$

from which it is apparent that

$$T_1 T_2 \frac{d^3 y}{dt^3} + (T_1+T_2) \frac{d^2 y}{dt^2} + \frac{dy}{dt} = Ke. \qquad \text{A-14}$$

The function h(y) has the form

$$h(y) = y(1 + cy^2). \qquad \text{A-15}$$

From equations A-15, A-11 and A-14 the mathematical model becomes

$$\frac{d^3 y}{dt^3} + \left(\frac{T_1 + T_2}{T_1 T_2} \right) \frac{d^2 y}{dt^2} + \frac{1}{T_1 T_2} \frac{dy}{dt} + y \left(\frac{K}{T_1 T_2} + \frac{KC}{T_1 T_2} y^2 \right) = \frac{K}{T_1 T_2} r(t) \qquad \text{A-16}$$

which is of the form of II-1.

The constants in equation A-16 were selected so that the equation under investigation is

$$\frac{d^3 y}{dt^3} + 3 \frac{d^2 y}{dt^2} + 2 \frac{dy}{dt} + 3y(1-0.05y^2) = 3r(t). \qquad \text{A-17}$$

The dependent variable, y, is assumed to range in magnitude between 0 and 4. The corresponding coefficients of y are tabulated for some typical values.

TABLE I

TYPICAL COEFFICIENT VARIATIONS

y	coefficient
0	3.
$\pm$ 1/2	2.9625
$\pm$ 1	2.85
$\pm$ 3/2	2.6625
$\pm$ 2	2.4
$\pm$ 5/2	2.0625
$\pm$ 3	1.65
$\pm$ 4	0.6

In each case the cubic equation was factored by a digital computer with roots as shown. These roots lie on the root ensemble which is

TABLE II

CHARACTERISTIC ROOTS OF THE LINEARIZED EQUATIONS

y	s_1	s_2	s_3
0	-2.6717000	-.1641+j1.047	-.1641-j1.047
$\pm$1	-2.6510980	-.1744+j1.022	-.1744-j1.022
$\pm$2	-2.5854778	-.2073+j .9409	-.2073-j .9409
$\pm$3	-2.4596040	-.2702+j..7732	-.2702-j .7732
$\pm$4	-2.2211968	-.3894+j .3442	-.3894-j .3442

illustrated by Figure 7.

Nonlinear Speed Control System

The nonlinear speed control system of Figure 8 represents a commonly encountered forward transmission device. The motor is assumed to have a polar moment of inertia, J_m, which in combination with load inertia, J_l, results in a total inertia of

$$J = J_m + J_l, \qquad \text{A-18}$$

Friction is considered to be of the viscous variety. The speed-torque curves of Figure 9 illustrate a speed-torque relationship of

$$T = (-1/2)\omega^2 + E_a \qquad \text{A-19}$$

The equation of motion is then

$$T = (-1/2)\omega^2 + E_a = J\frac{d\omega}{dt} + B\omega \qquad \text{A-20}$$

where B is the viscous friction constant. Equation A-20 may be re-written in terms of E_i as

$$KE_i = J\frac{d\omega}{dt} + \omega(B-1/2\omega). \qquad \text{A-21}$$

For purposes of illustration the constants have been selected so that

$$E_i = 1/2\frac{d\omega}{dt} + \omega(3-1/2\omega) \qquad \text{A-22}$$

The root ensemble is shown in Figure 10.

APPENDIX B

THE NONLINEAR OSCILLATOR

The circuit of Figure 17 is assumed to have a nonlinearity in the electron tube which is described by the relationship

$$i_p = g_m \left[e_g - \frac{1}{3E_s^2} e_g^3 \right] \qquad \text{B-1}$$

where g_m is the transconductance of the tube and E_s is the saturation voltage. This equation is plotted in Figure 18. The Kirchhoff voltage law equation of the grid circuit is

$$L_g \frac{di_g}{dt} + Ri_g + \frac{1}{c}\int i_g dt - M \frac{di_p}{dt} = 0. \qquad \text{B-2}$$

The voltage across the capacitor is

$$\frac{1}{c}\int i_g dt = e_g \qquad \text{B-3}$$

Combining equations B-1, B-2, and B-3 the result is

$$L_g c \frac{d^2 e_g}{dt^2} + Rc \frac{de_g}{dt} + e_g - Mg_m \left[\frac{de_g}{dt} - \frac{1}{3E_s^2} \frac{d(e_g^3)}{dt} \right] = 0. \qquad \text{B-4}$$

If $u = e_g/E_s$ equation B-4 may be rewritten as

$$\frac{d^2 u}{dt^2} - \left(\frac{Mg_m}{L_g C} - \frac{R}{L_g} \right) \frac{du}{dt} + \frac{Mg_m}{L_g C} 3u^2 \frac{du}{dt} + \frac{1}{L_g C} u = 0 \qquad \text{B-5}$$

or

$$\frac{d^2 u}{dt^2} - b \frac{du}{dt} + d \cdot 3u^2 \frac{du}{dt} + au = 0. \qquad \text{B-6}$$

Equation B-6 may finally be simplified by letting $x = (\sqrt{3d/b}\ )\ u$ to

$$\frac{d^2x}{dt^2} - b(1-x^2)\frac{dx}{dt} + ax = 0. \qquad \text{B-7}$$

For the particular example of Chapter III the values of b and a are $b = 0.8$ and $a = 1$. The root ensemble is shown in Figure 19.

Appendix C presents a Fortran listing of the program used to compute autonomous response of the oscillator. The results of the calculations are presented as Figures 20 and 21.

APPENDIX C

AUTONOMOUS RESPONSE PROGRAM FOR NONLINEAR OSCILLATOR

```
5       READ,T1,DIV,X,DX,N
        SUM1=0.
        ERR=0.
        T=T1
        DEL=0.
        DX1=ABS(DX)
        L=0
        TYPE,SUM1,X,DX,SUM1
35      RAD=4.-0.64*((1.-X**2)**2)
        L=L+1
        RE=0.4*(1.-(X**2))
        IF(RAD)250,200,50
50      OMEGA=0.5*SQR(RAD)
        DEN=((DX/X)-RE)
        PHI=ATN(OMEGA/DEN)
        IF(DEN)70,75,75
70      PHI=PHI+3.1415926
75      A=(X/OMEGA)*SQR(OMEGA**2+DEN**2)
        ANG=(OMEGA*(T/DIV)+PHI)
        DXOLD=DX
        XOLD=X
        X=A*EXP(RE*T/DIV)*SIN(ANG)
```

```
      DX=A*EXP(RE*T/DIV)*(OMEGA*COS(ANG)+RE*SIN(ANG))
93    IF(X)95,300,95
95    SUM1=SUM1+T/DIV
      DX2=ABS(DX)
      T=T1
      IF(DX1-DX2)110,115,115
110   DX1=DX2
115   DEL1=DX1*(ABS(0.8*(1.-(X**2))-2.*RE))
      R=4.8
      IF(DEL-DEL1)130,135,135
130   DEL=DEL1
135   ERR=ERR*EXP(R*T/DIV)+(DEL/R)*(EXP(R*T/DIV)-1.)
      M=L/N
      IF(M)160,35,160
160   L=0
      TYPE,SUM1,X,DX,ERR
      IF(SUM1-T1)35,5,5
200   XOLD=X
      DXOLD=DX
      B1=X*(1.+(DX/X+1.)*T/DIV)
      B2=(DX-(DX+X)*T/DIV)
      X=B1*EXP(-T/DIV)
      DX=B2*EXP(-T/DIV)
      GO TO 93
250   RAD=-RAD
```

```
      RE2=SQR(RAD)
      A1=RE+0.5*RE2
      A2=RE-0.5*RE2
      A3=(A2*X/(A2-A1))*(DX/X-2.*RE+A2)
      A4=(X/(A1-A2))*A1*(DX/X-2.*RE+A1)
      A5=(X/(A1-A2))*(DX/X-2.*RE+A1)
      A6=(X/(A1-A2))*(DX/X-2.*RE+A2)
      DXOLD=DX
      XOLD=X
      DX=A4*EXP(A1*T/DIV)+A3*EXP(A2*T/DIV)
      X=A5*EXP(A1*T/DIV)-A6*EXP(A2*T/DIV)
      GO TO 93
300   X=XOLD
      DX=DXOLD
      T=2.*T1
      GO TO 35
      END
```

VITA

Buck Ferguson Brown

Candidate for the Degree of

Doctor of Philosophy

Thesis: SEQUENTIAL SOLUTIONS IN NONLINEAR CONTROL THEORY

Major Field: Electrical Engineering

Biographical:

Personal Data: Born at Monroe, Louisiana, October 22, 1932, the son of O. Wharton and Roberta F. Brown.

Education: Attended grade and high school in Monroe and Baton Rouge, Louisiana; graduated from Webb School, Bell Buckle, Tennessee, in June, 1951; received the Bachelor of Science degree with a major in Electrical Engineering from the Massachusetts Institute of Technology in June, 1955; received the Master of Science degree with a major in Electrical Engineering from the Oklahoma State University in May, 1959. The requirements for the Doctor of Philosophy degree were completed in May, 1964.

Professional Experience: Employed by Convair Division of General Dynamics Corporation in Ft. Worth, Texas, as an Aerophysics Engineer from April, 1955 to September, 1956, and again from June, 1957, to September, 1957. Duties consisted of preliminary design and test of the B-58 automatic control system.

Employed by the School of Electrical Engineering of the Oklahoma State University in Stillwater, Oklahoma, from September, 1956, to May, 1957, and employed again in September, 1957. Duties consisted primarily of undergraduate instruction in the areas of circuits and systems.

Professional Organizations: Registered Professional Engineer in Oklahoma; member of the Institute of Electrical and Electronics Engineers and Sigma Tau; professional member of Eta Kappa Nu.